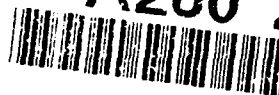


2

PL-TR-92-2250

AD-A260 232



MODELING DELAY-FIRED EXPLOSION  
SPECTRA AND SOURCE FUNCTION  
DECONVOLUTION AT REGIONAL DISTANCES

M. C. Chapman  
G. A. Bollinger  
M. S. Sibol

Virginia Polytechnic Institute  
and State University  
Department of Geological Sciences  
Blacksburg, Virginia 24061-0420

30 September 1992

DTIC  
ELECTE  
FEB 10 1993  
S E D

Final Report  
12 September 1990 - 30 November 1992

93-02437



57

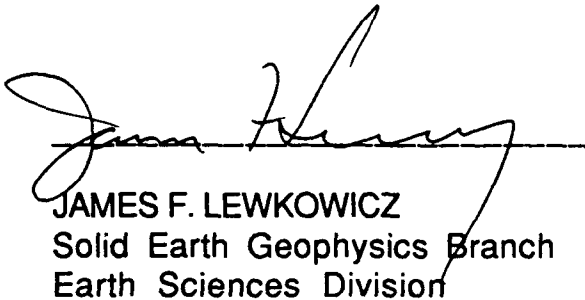
APPROVED FOR PUBLIC RELEASE; DISTRIBUTION UNLIMITED



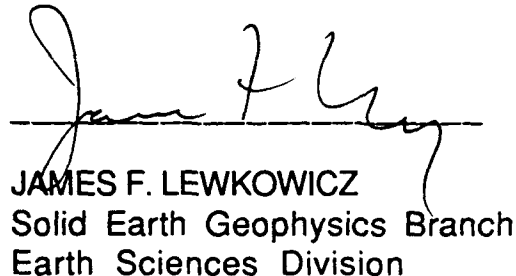
PHILLIPS LABORATORY  
Directorate of Geophysics  
AIR FORCE MATERIEL COMMAND  
HANSCOM AIR FORCE BASE, MA 01731-5000

The views and conclusions contained in this document are those of the authors and should not be interpreted as representing the official policies, either expressed or implied, of the Air Force or the U.S. Government.

This technical report has been reviewed and is approved for publication.



JAMES F. LEWKOWICZ  
Solid Earth Geophysics Branch  
Earth Sciences Division



JAMES F. LEWKOWICZ  
Solid Earth Geophysics Branch  
Earth Sciences Division



DONALD H. ECKHARDT, Director  
Earth Sciences Division

This document has been reviewed by the ESD Public Affairs Office (PA) and is releasable to the National Technical Information Service (NTIS).

Qualified requestors may obtain additional copies from the Defense Technical Information Center. All others should apply to the National Technical Information Service.

If your address has changed, or if you wish to be removed from the mailing list, or if the addressee is no longer employed by your organization, please notify PL/IMA, Hanscom AFB MA 01731-5000. This will assist us in maintaining a current mailing list.

Do not return copies of this report unless contractual obligations or notices on a specific document requires that it be returned.

REPORT DOCUMENTATION PAGE			Form Approved OMB No. 0704-0188	
<small>This report contains information which may be copyrighted. It is the property of the Government and is not to be distributed outside the Government. It is to be controlled, stored, handled, transmitted, and disposed of in accordance with the provisions of the Federal Acquisition Regulation (FAR) and the Department of Defense (DoD) Policy on the Control, Storage, Handling, Transmission, and Disposition of Information. It is to be controlled, stored, handled, transmitted, and disposed of in accordance with the provisions of the Federal Acquisition Regulation (FAR) and the Department of Defense (DoD) Policy on the Control, Storage, Handling, Transmission, and Disposition of Information.</small>				
1. AGENCY USE ONLY (Leave blank)		2. REPORT DATE 30 September 1992	3. REPORT TYPE AND DATES COVERED Final Report, 9/12/90 - 11/30/92	
4. TITLE AND SUBTITLE Modeling Delay-Fired Explosion Spectra and Source Function Deconvolution at Regional Distances			5. FUNDING NUMBERS F19628-90-K-0052 PR7600 PE62101F TA09 WUBB	
6. AUTHOR(S) M. C. Chapman G. A. Bollinger M. S. Sibol				
7. PERFORMING ORGANIZATION NAME(S) AND ADDRESS(ES) Virginia Polytechnic Institute and State University Department of Geological Sciences Blacksburg, Virginia 24061-0420			8. PERFORMING ORGANIZATION REPORT NUMBER	
9. SPONSORING MONITORING AGENCY NAME(S) AND ADDRESS(ES) Phillips Laboratory Hanscom AFB, Massachusetts 01731-5000  Contract Manager: James Lewkowicz/GPEH			10. SPONSORING MONITORING AGENCY REPORT NUMBER PL-TR-92-2230	
11. SUPPLEMENTARY NOTES				
12a. DISTRIBUTION AVAILABILITY STATEMENT Approved for public release; distribution unlimited			12b. DISTRIBUTION CODE	
13. ABSTRACT (Maximum 200 words)  The objectives of this study are to model the observed seismic spectra from large industrial explosions using information obtained from blaster's logs and to compare the explosion spectra with those of small earthquake signals from the same source region. The data were recorded on a short-period regional network at distances ranging from 180 to 400 km and have good signal-to-noise ratios at frequencies from 0.5 to 10 Hz.  The explosion amplitude spectra differ markedly from those of the earthquakes, by exhibiting strong time-independent amplitude modulations. This spectral modulation is directly attributable to the explosive charge geometry and firing sequence, and is largely independent of source-station path and recording site.  Modeling of the explosion source spectra shows that the major contributor to the modulated character of the spectra are amplitude minima at frequencies related to the total duration of the explosion sequence. Another important effect is amplitude reinforcement at low frequencies (e.g., 5 Hz) due to the comparatively long delay (0.2 sec) between the firing of individual rows of explosives. These features dominate both Pg and Lg amplitude spectra at frequencies less than 7 Hz. Accurate				
14. SUBJECT TERMS Industrial Explosions, Earthquakes, Source Spectra, Deconvolution			15. NUMBER OF PAGES 52	
			16. PRICE CODE	
17. SECURITY CLASSIFICATION OF REPORT Unclassified	18. SECURITY CLASSIFICATION OF THIS PAGE Unclassified	19. SECURITY CLASSIFICATION OF ABSTRACT Unclassified	20. LIMITATION OF ABSTRACT SAR	

modeling of the observed spectra at frequencies greater than a few Hertz requires that the azimuth of the recording site be taken into account. Also, the spectra at higher frequencies become sensitive to random variations in the firing times of any of the various subexplosions.

A deconvolution method based on low-time cepstral gating is tested, using the Lg phase from explosions and regional earthquakes. The deconvolution resolves the total duration and row delay intervals of an explosion with known firing sequence. In contrast, the deconvolved earthquake signals are simple and impulsive, and are readily distinguishable from all the deconvolved explosion signals. A limitation of the deconvolution process arises due to the assumption of a minimum phase delay source time function. Explosions employing constant row delay intervals are accurately deconvolved; however, complex explosion sequences with irregular firing patterns suffer from phase distortion in the deconvolution.

## CONTENTS

Introduction.....	1
Explosion Spectral Modulation.....	2
Data.....	4
Observed Spectra Versus Theoretical.....	6
Earthquake Spectra.....	10
Source Function Deconvolution.....	11
Conclusions.....	14
References.....	16
Figures.....	18

Accession For	
NTIS CRA&I	<input checked="" type="checkbox"/>
DTIC TAB	<input type="checkbox"/>
Unannounced	<input type="checkbox"/>
Justification	
By	
Distribution /	
Availability Codes	
Dist	Avail and/or Special
<b>A-1</b>	

## INTRODUCTION

Recent studies have demonstrated that the practice of delay firing commonly used for industrial explosions often produces observable modulations in the amplitude spectra of regional seismic signals that are not observed in earthquakes (Baumgardt and Ziegler, 1988; Smith, 1989; Hedlin et al., 1989; Baumgardt and Young, 1990; Hedlin et al., 1990). The form of the delay-fired explosion spectrum depends upon, among other factors, the spatial pattern of the charges, the variation in charge sizes, the delay time intervals between the firing of individual charges and the azimuth of the recording station from the source. Because single event sources such as smaller earthquakes or nuclear tests tend not to produce modulated source spectra, the observation of significant spectral modulations could provide a useful discriminant. However, path and receiver effects may complicate the situation. For example, the spectra of the regional seismic phases Pn, Pg, Sn and Lg can be influenced by the structure of the crustal waveguide and the anelastic absorption process will diminish spectral enhancements at high frequencies. The resonance effects of near surface, low velocity material near the source and near the receiver also can, in principle, introduce spectral modulations.

In this study, we examine the spectra recorded at near regional distances from large surface mining explosions and compare them with theoretical spectra derived on the basis of information contained in the blaster's logbooks. Additionally, we compare the explosion signals with those of some small earthquakes in the same source region, featuring similar propagation paths to the recording stations. We study the cause of the observed modulations in the explosion spectra, the effect of different source-station propagation paths on the spectra, and the spectral differences observed between the explosions and the earthquakes.

Using the theoretical source as a basis for comparison, we also test the utility of a deconvolution technique to recover the explosion source-time function from the recorded Lg phase.

## EXPLOSION SPECTRAL MODULATION

Generally, surface mine or quarry blasting operations employ explosive charges in holes that are arranged spatially in one or more rows. The individual charges are usually fired in a time sequence designed to achieve objectives such as proper rock breakage, reduction of fly rock, directed movement of the fractured rock mass, and reduced levels of ground motion. The time intervals (delays) between the individual subexplosions may be on the order of a few milliseconds to hundreds of milliseconds, depending on the application (Langefors and Kihlstrom, 1963; E.I. du Pont de Nemours & Co., 1978). For large mining explosions, similar to those studied here, a variety of different delays may be employed.

Baumgardt and Ziegler (1988), Smith (1989) and Hedlin et al. (1990) discuss the origin of spectral modulations in regional recordings of industrial explosions. Assuming that the explosion source-time function is a linear superposition of individual subexplosions (Stump and Reinke, 1988), we can model the explosion source by convolving a source wavelet  $S(t)$ , representing the time series due to the firing of a single charge, with an impulse series  $W(t)$ . In addition to the firing times and amplitudes of the subexplosions,  $W(t)$  incorporates the spatial distribution of the charge holes, the azimuth of the receiver and the wave velocity of the material. The source-time function,  $A(t)$ , for an explosion with  $n$  subexplosions observed at distances large in comparison to the dimension of the charge layout, is given by

$$A(t) = S(t) * W(t), \quad (1)$$

where

$$W(t) = \sum_{j=1}^n \alpha_j \delta(t - \tau_j), \quad (2)$$

and

$$\tau_j = \tau_j - (x_j \sin\theta + y_j \cos\theta)/V. \quad (3)$$

Here,  $\delta(t)$  is the delta function,  $\tau_j$  is the time of the  $j$ 'th subexplosion defined relative to the time of the initial subexplosion,  $x_j$  and  $y_j$  are the coordinates of the  $j$ 'th subexplosion in a coordinate system with origin at the location of the initial subexplosion. The constant  $\alpha_j$  represents the amplitude of the subexplosion. The azimuth  $\theta$  from origin to recording station is measured clockwise from the Y axis and  $V$  is the phase velocity. The amplitude spectrum  $A(\omega)$  of the source-time function is given by

$$A(\omega) = |S(\omega)W(\omega)|, \quad (4)$$

$$\text{where} \quad W(\omega) = \sum_{j=1}^n \alpha_j \exp(i\omega\tau_j') \quad (5)$$

Consider a simple case where a row of 10 holes with equal charges is fired sequentially from one end with a constant delay ( $\tau_j - \tau_{j-1}$ ) of 25 msec (Figure 1). For simplicity, assume  $S(t) = \delta(t)$ , a hole spacing ( $x_j - x_{j-1}$ ) of 4 meters and a velocity  $V$  of 3000 m/sec. The modulation of  $A(\omega)$  in this case, regardless of station azimuth  $\theta$ , involves two dominant effects. The first is amplitude reinforcement due to the constant time intervals (delays) between subexplosions. This reinforcement occurs at frequencies which are approximately integer multiples of the inverse delay interval. The second effect is spectral "scalping," characterized by amplitude minima at frequencies given approximately by integer multiples of the inverse duration of the explosion sequence. In the case for  $\theta = 0$  deg, the resulting spectrum is exactly that of the delay time series, with spectral reinforcements at 0, 40, 80 ... Hz, and spectral minima at 4, 8, 12 ... Hz (Fig. 1b). For  $\theta = 90$  deg, the apparent delays between the explosions (as seen from the station) are shortened by a Doppler-like effect, due to the progression of the shotpoint in the direction of the receiver, and the finite wave velocity. Hence, the spectral reinforcements and minima appear at higher frequencies (Fig. 2a). The opposite effect happens for a receiver on an azimuth in the opposite direction: the reinforcements and spectral minima are shifted to lower frequencies. In actual



practice, there may be significant variation in individual delay times, due to variations in the lengths and firing rates of detonating cords and blasting caps. This type of variation serves to reduce the amplitudes of the higher frequency reinforcement harmonics, and effectively "fills in" the spectral minima (Stump et al., 1989). Figure 2b shows the spectrum resulting from the previous case ( $\theta = 0$  deg) when a random error with zero mean and standard deviation equal to 10% of the mean delay time is added to the times of the subexplosions. This "whitens" the spectrum by reducing the amplitude of the high frequency peak at 80 Hz and filling up the high frequency minima. Note that the effect of station azimuth and random variation of firing times is minimal for the low frequency part of the spectrum.

Real explosions often incorporate several rows of charge holes which may be "decked" (i.e., multiple delays and charges for upper and lower parts of the same hole). The firing of multiple rows is generally done sequentially, with relatively large delays between rows so as to allow time for the fractured rock mass to move away from the newly created free face. These row delays may produce important amplitude reinforcements at relatively low frequencies. Figure 2c shows the time series for a case where four rows of 10 holes each are fired with 0.11 sec delays between rows. As in the previous case, the delays between firings of adjacent holes in a row is 0.025 sec, and the azimuth  $\theta$  is 0 deg. The row delays produce additional amplitude reinforcements at  $n/0.11$  Hz or 9.1, 18.2, 27.3 Hz... etc., and the longer duration of the explosion sequence (0.58 sec) produces a "scalloping" effect with amplitude minima more closely spaced in frequency, compared to the previous case for a single row of charges (Fig. 2d).

## DATA

The data set is derived from digital waveforms recorded by the Virginia Regional Seismic Network. Figure 3a shows the locations of the network stations, along with the locations of four explosions and the epicenters of two natural earthquakes. The network utilizes 1 Hz seismometers. The analog seismic signals are transmitted to a central recording facility by FM telemetry and

digitized at 100 samples/sec. The time series of these six events as recorded at station WMV are shown in Figure 3b.

The explosions studied here were fired to remove the overburden from coal seams. We obtained copies of the blaster's logs and used this information to model the explosion amplitude spectrum by means of equations 1 through 5.

The detail of information contained in the logs varied among the individual explosions. However, in all cases, the nominal firing time of each charge could be ascertained. Other pertinent information contained in the logs included the distance between rows (burden) and between holes in a row (spacing), the types of millisecond delay connectors used (9, 17, 42 and 200 msec, in various combinations), the types of downhole delay blasting caps (450 or 500 msec), the total charge weight used for each hole and the maximum weight per delay period. Important ambiguities in the logs involve the distribution of charge weight within some of the decked holes for three of the four explosions: also, details concerning the use and arrangement of high velocity detonating cord and/or shock tubing (a lower velocity detonation device) were not available. Additionally, only nominal firing times for the charges are available from the logbooks: Stump et al. (1989) report that the standard deviation of mean firing times of common commercial initiation devices is 5 msec. The main charge was a mixture of ammonium nitrate and fuel oil, initiated by a small primer charge using nonelectric downhole blasting caps. The copies of the blasting logs and other information, such as the orientation of the charge pattern with respect to North, were kindly furnished by the Kentucky Department of Mines and Minerals (written communication).

Figure 4a shows the charge pattern for Explosion 1. It consisted of four rows of decked charges with the initiation point in the center of the row adjacent to the free face. The burden and spacing were 8.8 and 11 meters, respectively. The majority of delays used between holes in a given row were 17 msec, and each row was delayed 200 msec. The 56 charge holes were 31 cm in diameter and were drilled to a depth of 34.1 m. The lower part of each hole was loaded with 1877 lbs of explosive. The bottom charge was separated from the top charge of 2248 lbs of explosive by a 3 meter deck of drill cuttings. The top charge was fired using a 450 msec delay

nonelectric cap: the bottom charge was delayed 50 msec by using a 500 msec nonelectric cap.

Figure 4b shows the nominal delay time series  $W(t)$  for a station azimuth of 307 deg.

The remaining three explosions involved in the study were also multi-row, decked designs similar to Explosion 1. However, the distribution of charge weights between upper and lower decks in some of the rows was not specified. Figure 5 shows the model time series constructed for Explosions 2 through 4, with charge weight distributed as suggested in the blaster's logbook.

### OBSERVED SPECTRA VERSUS THEORETICAL

The explosions studied here produced time independent spectral modulations. This phenomenon has been noted previously (see, e.g., Baumgardt and Ziegler, 1988) from industrial explosions, and is an indication that the modulations are source related and not due to multipathing. It is most apparent when the data are displayed in a sonogram or time-frequency plot wherein the spectral content of the entire signal is plotted as a function of time.

Figure 6a shows a sonogram for Explosion 2. It was created using an approach similar to that of Hedlin et al. (1989). Instrument corrected acceleration power spectra were computed using non-overlapping five second windows, for times beginning well before the signal onset and extending into the signal coda. The spectra were detrended and amplitude normalized by subtracting a second degree polynomial fitted by least squares to the logarithms of acceleration power. Effects of noise were minimized by contouring only those values that exceed the pre-signal noise levels by a factor of 5. Note that the spectral peaks persist throughout the signal, from P onset to well into the Lg coda.

In Figures 7 through 10, we compare the acceleration amplitude spectra of Lg and Pg with model spectra for each of the four explosions. The tick marks in Figure 3b indicate the time windows used for analysis. The Lg spectra were derived from 20 sec time windows and were smoothed with a 4 point moving average. The Pg windows were 6 sec in duration, and smoothing was done with a 2 point moving average. All spectra have been corrected for instrument response

and anelastic attenuation. The assumed Pg and Lg quality factor is  $Q = 811f^{0.42}$ , derived from observations of regional earthquake Lg coda decay at the same network stations used in the present study (Chapman and Rogers, 1989). However, the validity of this attenuation model for surface sources has not yet been tested. Also, it is possible that coda Q values are not appropriate for Pg.

Figure 7a shows the Lg spectrum recorded at WMV from Explosion 1, along with the pre-P noise background. Both spectra were calculated using 20 second time windows, and smoothed using a 4 point moving average. Note that the signal/noise ratio exceeds 2 at frequencies less than 15 Hz. This station, along with station VWV, gave the best signal/noise ratios. Figure 7b shows the vertical component Lg acceleration spectra (20 sec windows) at stations WMV, VWV and CVL, in comparison with the model acceleration spectrum for Explosion 1. The observed spectra are plotted at frequencies where the signal/noise ratio exceeds 2. Note the good agreement between observed and model spectra at frequencies less than about 7 Hz. The similarity of spectra at the three stations clearly demonstrates that the significant modulations at low frequency are path and site independent.

Figure 7c shows the Pg acceleration spectrum from Explosion 1 at WMV, VWV and CVL. Agreement between the Pg spectra and the model spectrum is not as good as for Lg. This may be due in part to the lower signal/noise ratios for Pg compared to Lg.

A potential for significant error in the modeling of the high frequency spectrum exists because of uncertainty involving the detonation velocity and arrangement of the surface and downhole shock tubing and/or detonating cord. The logs did not specify which type of device was used to initiate the explosions. It is possible that both types of initiation device were employed: e.g., high velocity detonating cord can be used on the surface, with lower velocity shock tubing used to initiate the downhole caps. Modeling of the effect shows little impact on the spectra at frequencies less than 20 Hz if the effective between-charge detonation velocity is in excess of 6000 m/sec. It appears that the time delays introduced from this source have a minor effect on the observed amplitude spectra at the relatively low frequencies (7 Hz and less) where we have large signal/noise ratios.

The theoretical model assumes a Brune (1970)  $\omega^2$  acceleration amplitude spectrum with corner frequency  $\omega_c$  for the source wavelet: hence, in equation (4),

$$|S(\omega)| = \frac{\omega^2}{1 + (\frac{\omega}{\omega_c})^2} \quad (6)$$

The simple  $\omega^2$  source spectrum was chosen for convenience. Because of uncertainties regarding path attenuation effects, use of a more complex model seems unjustified. Figure 8 shows the observed amplitude spectra of both Lg and Pg at stations WMV and VWV in comparison with model spectra constructed for a range of corner frequency values. Although somewhat equivocal, it appears that the Lg spectra imply a lower corner frequency than the Pg phase. Values of 3 Hz for Lg and 10 Hz for Pg were used to construct the model spectra shown in Figure 7. Note however, that in Figure 8, the corner frequencies for both phases appear somewhat higher for station WMV than for VWV. This site dependent effect is also observed in the spectra of two earthquakes recorded at VWV and WMV, suggesting that the low apparent corner frequencies, especially for Lg, are not due to the explosion source, but rather represent a propagation phenomenon, that may involve recording site response. Single charge explosions of the size studied here are expected to produce source spectra with corner frequencies considerably higher than 10 Hz. Stump et al. (1991) modeled the near field spectra of cylindrical charge explosions in hard rock using a modified Mueller and Murphy (1971) source model. They suggest that the equivalent elastic radius is approximately equal to the length of the charge column, with a 150 lb charge of length 18 m producing a spectrum with corner frequency near 50 Hz. Although the charge weights involved in the explosions studied here greatly exceed 150 lbs, the length of the charges are similar to those studied by Stump et al. (1991).

Other parameters in the theoretical model include the charge weight - amplitude scaling relations, phase velocity, and receiver azimuth. Because not all holes were loaded to the same charge weight, the nature of the amplitude - charge weight relationship will affect the modulation

pattern of the explosion spectrum. In the explosion designs studied here, this effect arises largely due to differences in charge weight between the upper and lower decks in each row of explosives. To examine the sensitivity of the model spectra to the amplitude - charge weight scaling, we compared the model spectra assuming that amplitude scales in direct proportion to charge weight, as opposed to the cube root of the weight. This range of values includes the results of Medearis (1979) who studied peak time domain and spectral amplitudes of industrial explosions. Figure 9a shows the results of this comparison. Other than a broadband change in the spectral level, the effect on the modulation pattern of the model spectrum for Explosion 1 is very minor.

The effect of phase velocity on the spectrum of Explosion 1 is shown in Figure 9b. For that design, the modulation pattern at frequencies less than 20 Hz is virtually independent of velocities in excess of 3000 m/sec, the assumed shear wave velocity of the Paleozoic sandstones and shales known to be present in the mine locale. However, a velocity of 1500 m/sec produces a substantially different modulation pattern at frequencies higher than 10 Hz. Clearly, the degree to which the phase velocity influences the spectrum of the explosion depends upon the azimuth of the receiver and upon the charge spacing and delay times. For the four explosions modeled in this study, the phase velocity appears not to be a critical parameter at frequencies of 15 Hz and less, where signal/noise ratios are adequate.

Figure 9c shows the effect of station azimuth upon the model spectrum of Explosion 1. The assumed phase velocity is 3000 m/sec. Although the very low frequency spectrum (less than 5 Hz) is only slightly affected by a  $\pm 90$  deg variation in station azimuth for this explosion design, the spectrum at higher frequencies is strongly influenced by the azimuth, and it is an important parameter for modeling the explosion spectrum at frequencies less than 15 Hz.

The Lg acceleration spectra for Explosions 2, 3 and 4 are shown in Figure 10. As in the previous example, the spectra were smoothed and plotted at frequencies where the signal/noise is greater than 2. Although the exact charge weight distribution is in question for these explosions, the overall shape and the frequencies of peaks and troughs in the observed spectra match those of

the model spectra well. Again, the model Lg spectra source wavelet corner frequency is 3 Hz, and the velocity assumed is 3000 m/sec.

The appearance of the spectra from all four explosions at frequencies less than about 7 Hz is readily explained in terms of two effects. The most obvious aspect of the spectra are the amplitude minima at approximately 1.2, 2.3 and 3.4 Hz. These are directly related to the apparent duration of the explosion sequence and coincide with the amplitude nulls in the spectrum of a square wave time function of duration T sec. The frequencies of the amplitude nulls are given by  $n/T$ , where  $n=1,2,3,\dots$  etc. The apparent duration T of Explosions 1 through 4 are 0.90, 0.93, 0.85 and 0.84 seconds, respectively.

The other major aspect of the observed spectra is the persistent strong amplitude peak near 5 Hz. This peak is the result of reinforcement due to a nominal row delay of 0.2 sec used in all of the explosions.

## EARTHQUAKE SPECTRA

The two earthquakes which occurred in eastern Kentucky provide an opportunity to compare spectra from known explosions and earthquakes over similar source-station paths (Figure 3).

Figure 11 compares the Lg and Pg path corrected acceleration spectra from both earthquakes and Explosion 1. The time windows used for station WMV are indicated in Figure 3. Note that for the larger earthquake (#2), the maximum amplitude part of the Lg phase at WMV was clipped, and in that case, the Lg spectrum was derived from a window somewhat later in the Lg coda. The spectra were smoothed as previously described and amplitudes scaled so that the Lg and Pg spectra overlap at high frequency.

The modulations apparent in the earthquake spectra are smaller in amplitude than those of the explosion spectra at low frequencies, and the Pg and Lg modulations in the explosion spectra are correlated, whereas those in the earthquake spectra are not. This lack of temporal stationarity

of the earthquake spectral modulation pattern results in sonogram plots that appear essentially random, without the strong time-independent spectral bands of the explosion sonogram (Figure 6).

## SOURCE FUNCTION DECONVOLUTION

In the following, we test a technique involving cepstral filtering to recover the source-time function of the explosion signals (Ulrych, 1971; Tribolet, 1979). We assume that the recorded seismic signal is a convolution of the source time series with a random sequence representing the impulse response of the transmission path. Under these assumptions, the source in the cepstral domain is confined to small times (small quefrency values). Hence, the effects of the transmission path can be reduced by suppressing large time values of the complex cepstrum. A difficulty arises in computing the complex cepstrum, because a continuous phase function must be defined. This generally requires that the principle values of the phase spectrum be "unwrapped". Various approaches to the problem are discussed by Tribolet (1977). However, if the source-time function is "minimum phase" the continuous phase function can be defined uniquely as the Hilbert transform of the logarithm of the amplitude spectrum.

Let  $x(t)$  be the recorded time series and  $X(\omega)$  represent its Fourier transform. Then, in polar form,

$$X(\omega) = |X(\omega)| \exp\{i\Theta(\omega)\} \quad (7)$$

where  $\Theta(\omega)$  is the phase spectrum. The Fourier transform of the complex cepstrum is given by

$$S(\omega) = \ln \{X(\omega)\} = \ln|X(\omega)| + i\Theta(\omega) \quad (8)$$

where  $\Theta(\omega)$  is a continuous function of frequency. The complex cepstrum,  $s(t)$ , is obtained via the inverse Fourier transform. Assuming  $x(t)$  to be minimum phase, the continuous phase is given by



$$\Theta(\omega) = H\{\ln|X(\omega)|\} \quad (9)$$

where  $H$  indicates the Hilbert transform. The cepstral filtering is accomplished by

$$s'(t) = a(t) s(t), \quad (10)$$

where

$$a(t) = 0, t < 0$$

$$a(t) = 1, 0 \leq t \leq T$$

$$a(t) = 0, t > T$$

In the above,  $T$  represents the duration of the cepstral gate. The deconvolved time series is recovered by computing the direct Fourier transform of  $s'(t)$ , followed by exponentiation and inverse Fourier transformation.

An example of the process, using synthetic data, is shown in Figure 12a. The source function is represented by four acceleration pulses, equally spaced in time, with equal amplitudes. This source series is convolved with a random sequence, to simulate a recorded seismic signal, then deconvolved using the minimum phase assumption. In this example, the minimum phase deconvolution preserves the time intervals and amplitudes of the original source time series. This will not be the case in general, as shown in Figure 12b. The minimum phase deconvolution preserves the proper time intervals between source pulses only if the pulses are equally spaced in time. When that is the case, the process will give a useful result when the pulse amplitudes are nearly equal or else distributed such that the energy is concentrated early in the source time series. Many, if not most, large mining explosion designs incorporate shot patterns and explosion delay intervals which result in near constant time intervals between the firing of rows of explosions. As shown above, these row delays can strongly impact the low frequency spectra recorded at larger distances, and may be resolved using the process described above.

The data set used to test the deconvolution technique consisted of Explosion 1, described above, for which we have the most detailed information on the blast design. In addition to the two earthquakes described previously (Figure 3), we deconvolved the signals from an additional regional earthquake and three additional mining explosions, which originated at different mines. The locations of these events are shown in Figure 13.

Figure 14 shows the results of the minimum phase deconvolution for each network station from Explosion 1, as well as the network average deconvolution. In this and in all later examples, the time series analyzed consisted of 20 second duration windows, beginning with the onset of the Lg phase. The recorded data were instrument corrected to ground acceleration, and band-passed with 6-pole Butterworth filters with corner frequencies at 0.3 and 15 Hz. The duration of the cepstral gate was 1.0 second.

A model acceleration time series was constructed for Explosion 1 and is plotted for comparison with the network average deconvolution in Figure 15. The model time series incorporates a Brune source pulse with corner frequency 10 Hz, convolved with the firing sequence shown in Figure 4b. Anelastic attenuation was represented by  $\exp(-\omega t^*)$ , where  $t^*=0.04$ . As shown in Figure 4, this explosion design involving four rows of explosives with a constant row delay of 0.2 sec is clearly resolved in the deconvolved seismic data.

Figures 16, 17 and 18 show the deconvolutions obtained from Earthquakes 1, 2 and 3. Identical processing was performed on all events, as described above. Note that the earthquake deconvolutions indicate single, short duration source functions.

Figures 19, 20 and 21 show the deconvolution results for Explosions 5, 6 and 7 which occurred at different mines. Figure 22 compares the deconvolutions derived from all events shown in Figure 13. Information on the charge patterns and delay times used in Explosions 5 through 7 is lacking. However, like Explosion 1, Explosion 5 exhibits evidence for source multiplicity. The results for Explosions 6 and 7 are more ambiguous, but by analogy with the results obtained from Explosion 1, and in contrast to the results from the earthquakes, the deconvolutions for the other

explosions appear to exhibit evidence for source multiplicity and/or extended durations. Explosion 6 suggests a large delay period (approximately 0.4 sec).

## CONCLUSIONS

The surface mine explosions studied here produced signals at near regional distance featuring time independent spectral modulations of the type previously reported by Baumgardt and Ziegler (1988), Smith (1989), Hedlin et al. (1989), Baumgardt and Young (1990) and Hedlin et al. (1990). The dominant features of the modulation are independent of recording site and source-station path. In contrast, natural earthquakes which occurred in the mine locale exhibit much flatter acceleration spectra, with substantially larger high frequency amplitudes, and show no evidence of time independent spectral modulation.

The explosion spectra were successfully reproduced at low frequency using a simple model. The most obvious characteristics of the explosion spectra are amplitude minima controlled by the total duration of the explosion sequence, and amplitude reinforcement due to relatively long (0.2 sec) delays between the firing of multiple rows of explosives. The model spectra at low frequency are relatively insensitive to station azimuth and phase velocity. However, as frequency increases, the sensitivity of the models to station azimuth and to a lesser degree, phase velocity also increases. Additionally, any random variation in the firing times of subexplosions strongly affects the high frequency spectrum. Because of these complicating effects, and adequate signal/noise ratios limited to less than 15 Hz, resolution of source features other than total duration and the gross temporal pattern due to the 0.2 sec row delays was not possible. However, agreement between the model Lg spectra and the observations at frequencies less than approximately 7 Hz implies that for the study area at least, the Earth's transfer function for low frequency Lg waves is very simple: i.e., it acts primarily as a low pass filter in terms of amplitude response.

The Pg and Lg explosion spectra show similar amplitude modulations. The Lg spectra more closely matched the model spectra, but this may be due to larger Lg signal/noise ratios.

Interestingly, the Pg spectra appear to have relatively larger amplitudes at high frequency than do the Lg spectra. Recordings at smaller distances will be required to determine whether or not this observation indicates real differences in the source amplitude spectra of the two phases, rather than a path effect involving stronger attenuation of the Lg phase.

Deconvolution of the Lg phase by low-time cepstral gating effectively reveals source multiplicity in some large mining explosions recorded at near regional distances. The accuracy of the deconvolution procedure used here depends upon the phase characteristics of the source function. Minimum phase source series appear to be accurately preserved. Further work needs to be done to extend this result to source functions with mixed phase characteristics.

## REFERENCES

- Baumgardt, D. R. and K. A. Ziegler (1988). Spectral evidence for source multiplicity in explosions: Application to regional discrimination of earthquakes and explosions, *Bull. Seism. Soc. Am.* 78, 1773-1795.
- Baumgardt, D. R. and G. B. Young (1990). Regional seismic waveform discriminants and case-based event identification using regional arrays, *Bull. Seism. Soc. Am.* 80b, 1874-1892.
- Brune, J. N. (1970). Tectonic stress and the spectra of seismic shear waves from earthquakes, *J. Geophys. Res.* 75, 4997-5009.
- Chapman, M. C. and M. J. B. Rogers (1989). Coda Q in the Southern Appalachians, *Geophys. Res. Letters* 16, 531-534.
- E. I. du Pont de Nemours & Co. (1978). *Blasters' Handbook*, 16th Ed., du Pont Technical Services Section, Explosives Product Division, Wilmington, Delaware, 494 p.
- Hedlin, M. A. H., J. B. Minster and J. A. Orcutt (1989). The time-frequency characteristics of quarry blasts and calibration explosions recorded in Kazakhstan, USSR, *Geophys. J. Int.* 99, 109-121.
- Hedlin, M. A. H., J. B. Minster and J. A. Orcutt (1990). An automatic means to discriminate between earthquakes and quarry blasts, *Bull. Seism. Soc. Am.* 80b, 2143-2160.
- Langefors, U. and B. Kihlstrom (1963). *The Modern Technique of Rock Blasting*, John Wiley and Sons, New York.
- Medearis, K. (1979). Dynamic characteristics of ground motions due to blasting, *Bull. Seism. Soc. Am.* 69, 627-639.
- Mueller, R. A. and J. R. Murphy, J. R. (1971). Seismic characteristics of underground nuclear detonations: Part 1. seismic spectrum scaling, *Bull. Seism. Soc. Am.* 61, 1675-1692.
- Smith, A. T. (1989). High-frequency seismic observations and models of chemical explosions: Implications for the discrimination of ripple-fired mining blasts, *Bull. Seism. Soc. Am.* 79, 1089-1110.
- Stump, B. W. and R. E. Reinke (1988). Experimental confirmation of superposition from small scale explosions, *Bull. Seism. Soc. Am.* 78, 1059-1073.
- Stump, B. W., S. Reamer, D. Anderson, K. Olsen, and R. Reinke (1989). Quantification of explosion source characteristics from near source, regional and teleseismic distances, *U.S. Air Force Systems Command, Geophysics Laboratory Report GL-TR-89-0194*, ADA-216218.
- Stump, B. W., S. Reamer, K. G. Hinzen and G. Min (1991) Physical constraints on seismic waves from chemical and nuclear explosions, *Proceedings of 13th annual PL/DARPA seismic research symposium, 8-10 Oct., 1991*, 424-430, *PL-TR-91-2208*, ADA241325.
- Tribolet, J. M. (1977). A new phase unwrapping algorithm, *IEEE Trans. ASSP* 25, no. 2, 170-177.

Tribolet, J. M. (1979). *Seismic Applications of Homomorphic Signal Processing*, Prentice Hall, Englewood Cliffs, NJ, 195 p.

Ulrych, T. J. (1971). Application of homomorphic deconvolution to seismology, *Geophysics* 36, no. 4, 650-660.

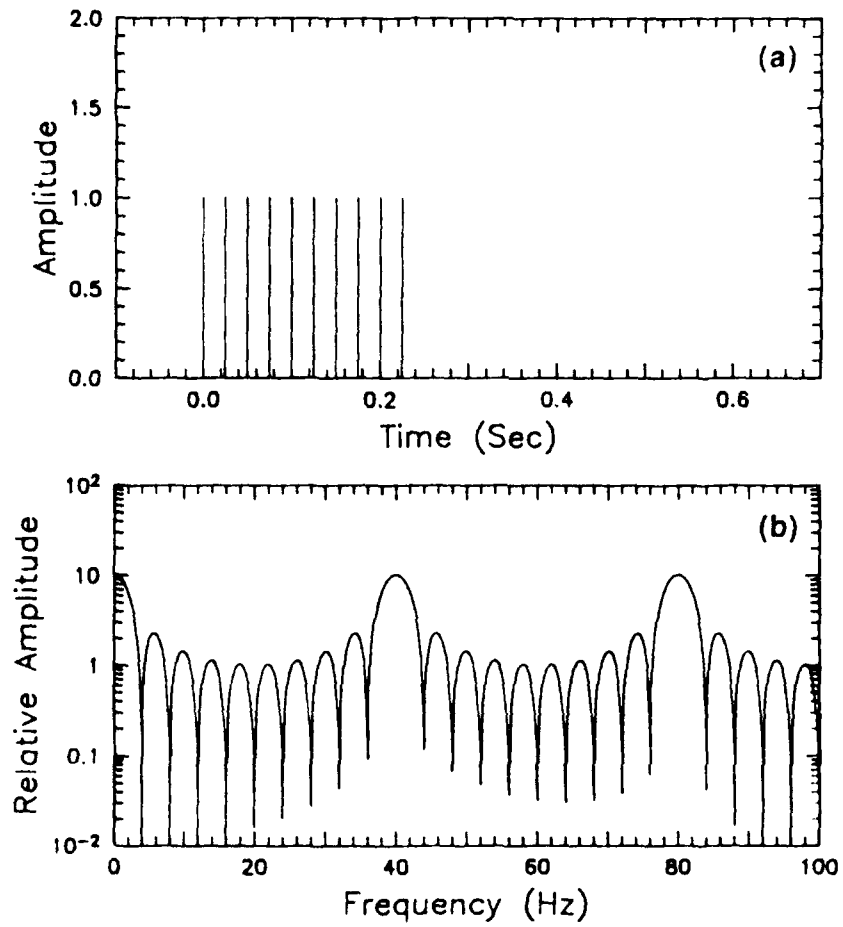


Fig. 1. (a) Time series of a single row of explosions, with station azimuth perpendicular to the row ( $\theta=0$  deg). (b) Corresponding amplitude spectrum.

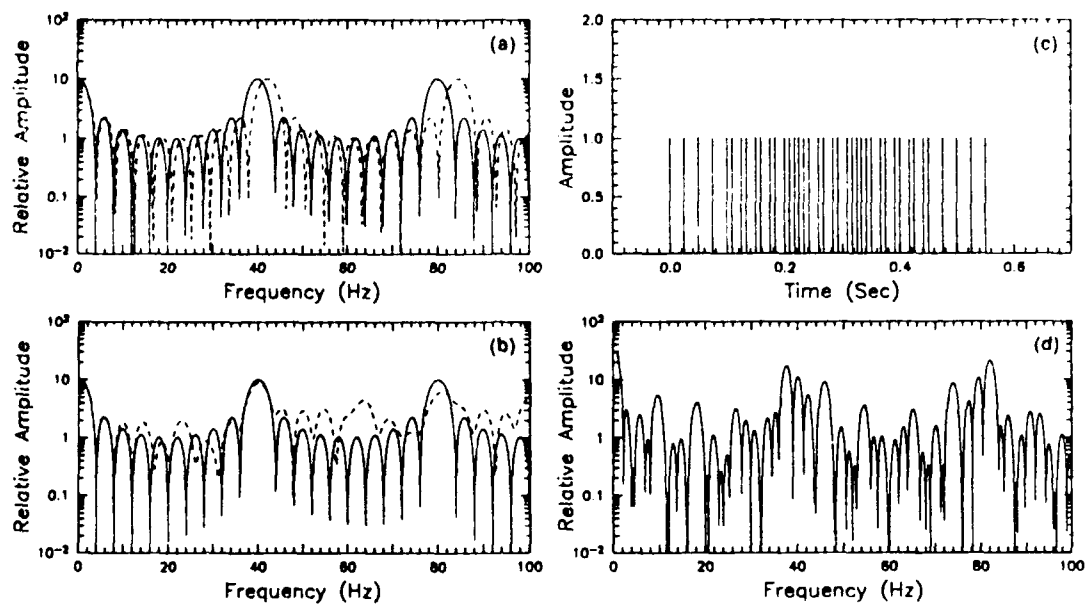


Fig. 2. (a) Spectrum corresponding to case where station azimuth is 90 deg. (b) Spectrum resulting from 10% random variation in delay times of individual explosions. In (a) and (b), the solid lines are as in Figure 1b. (c) Time series for 4 rows of explosions with 10 charges per row: azimuth  $q=0$  deg, phase velocity  $V=3000$  m/sec (d) Corresponding amplitude spectrum.



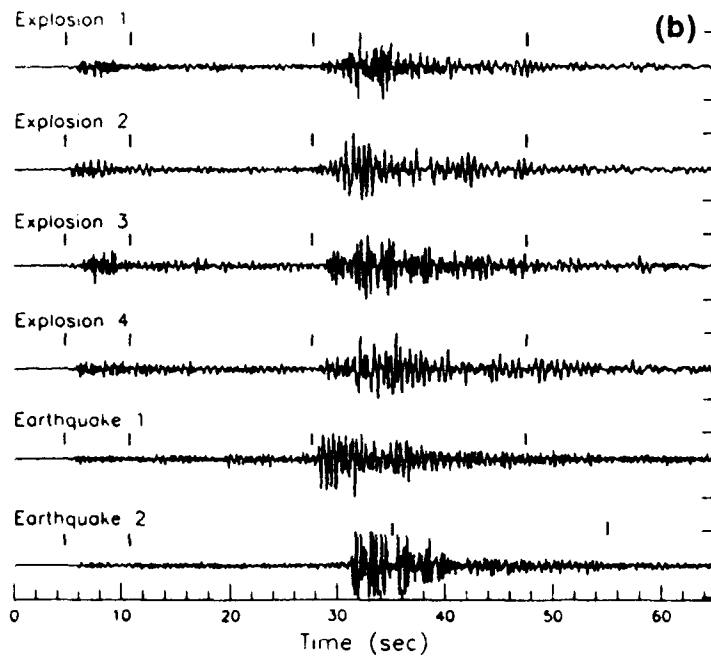
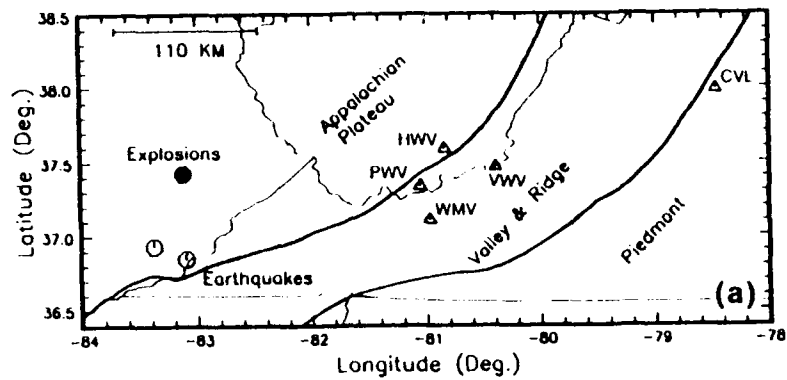


Fig. 3. (a) Location map showing network stations (open triangles) earthquake epicenters (open circles) and the location of four surface mine explosions (solid circle). (b) Vertical component seismograms from station WMV of the events involved in the study. Tick marks indicate time windows used for spectral analysis.

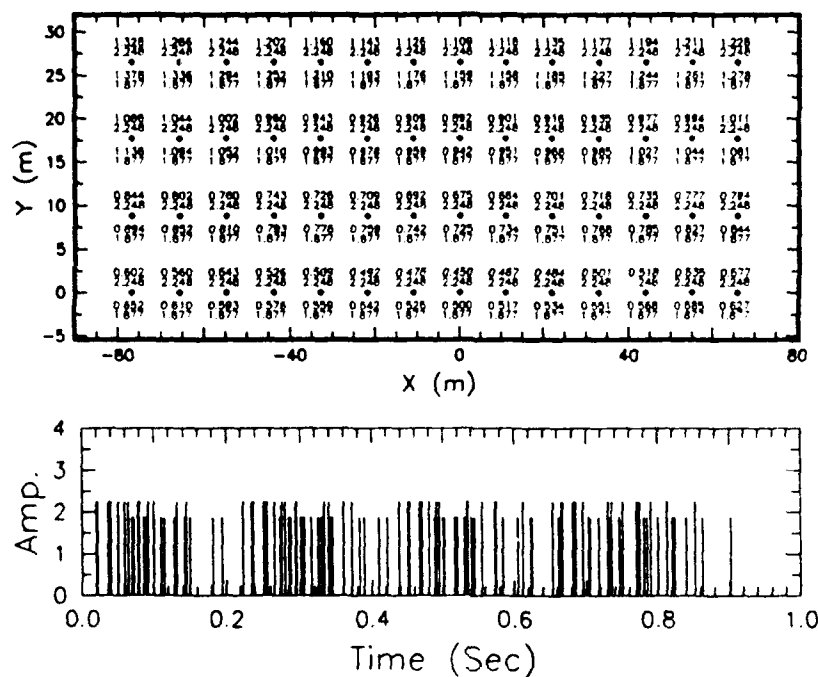


Fig. 4. (a) Charge pattern for Explosion 1 (plan view). Locations of each hole are indicated by small circles. Numbers above each circle indicate firing time (sec) of upper charge and charge weight (thousands of pounds), respectively. Numbers below circle refer to lower charge firing time and charge weight. (b) Time series of Explosion 1, assuming station azimuth 307 deg, and phase velocity 3000 m/sec. Amplitude is charge weight in thousands of pounds.

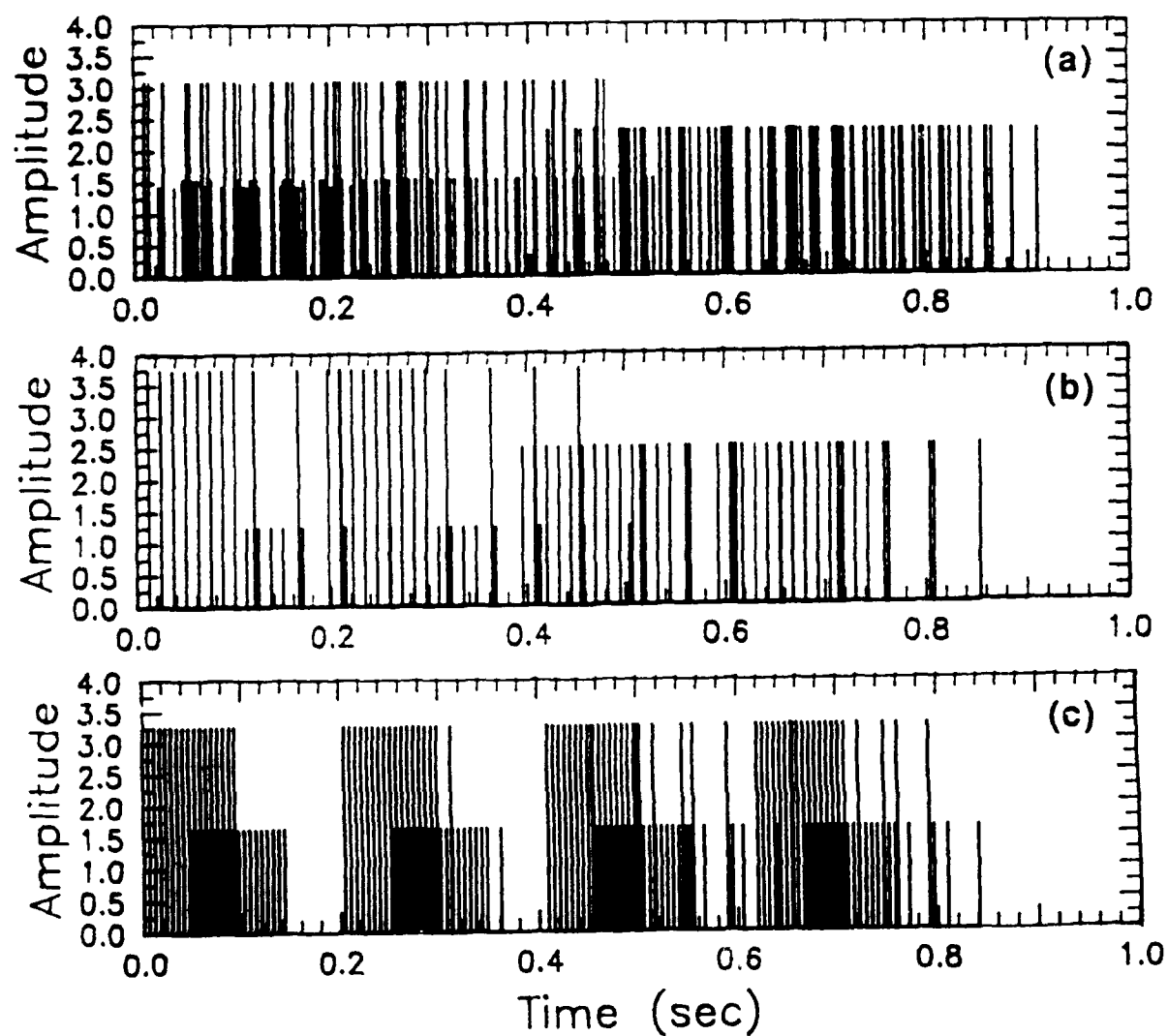


Fig. 5. Model time series developed for Explosions 2 (a), 3 (b) and 4 (c), assuming station azimuths of 327, 115 and 125 degrees, respectively. Amplitudes are charge weight in thousands of pounds.

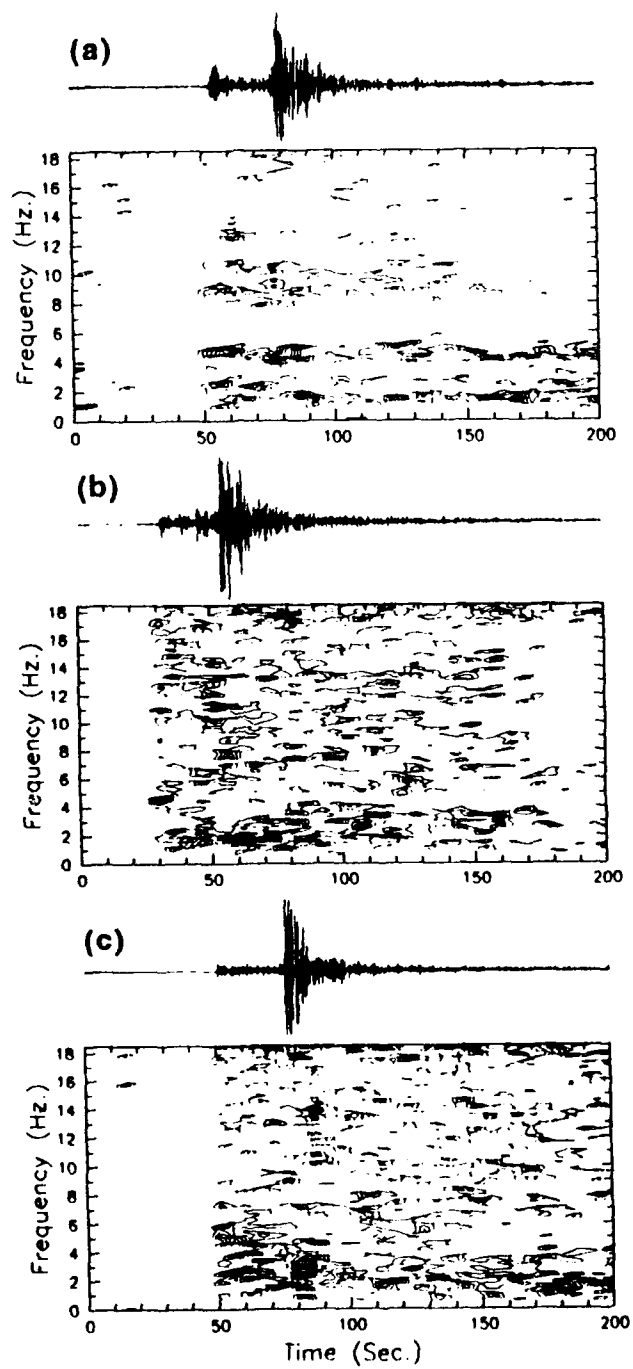


Fig. 6. Time series and sonograms for Explosion 2 (a), the November 27, 1987 Kentucky-Virginia border earthquake (b) and the August 17, 1990 Kentucky earthquake (c).

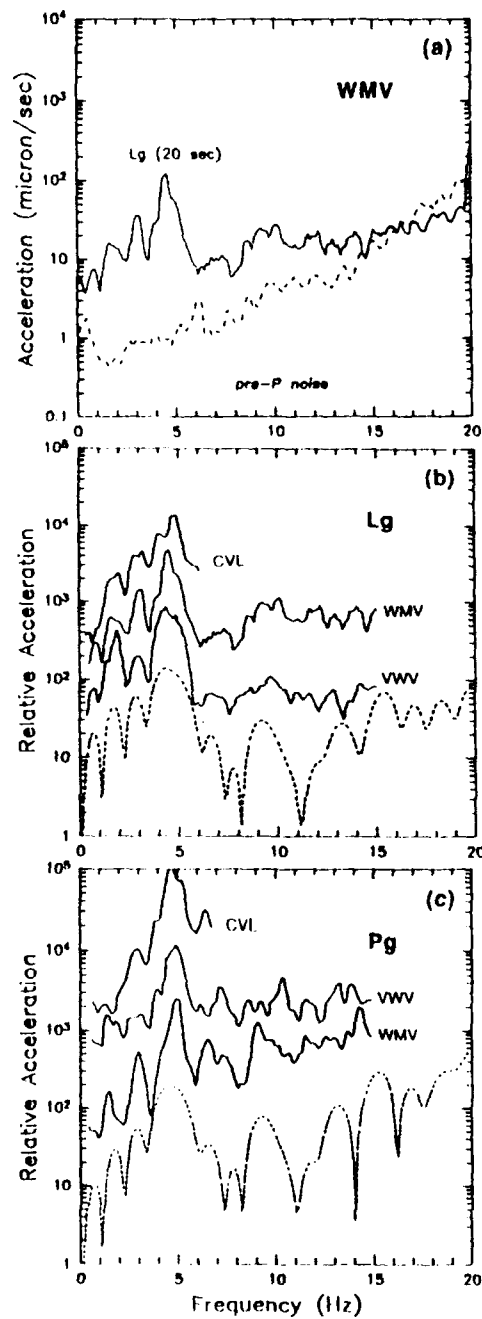


Fig. 7. (a) Vertical component Lg acceleration spectrum (solid) and pre-P wave noise spectrum (dashed) for Explosion 1. (b) Lg acceleration spectra for Explosion 1 (solid) (c) Pg acceleration spectra for Explosion 1 (solid). In (b) and (c), dashed lines show model spectrum, and amplitudes have been scaled for separation.

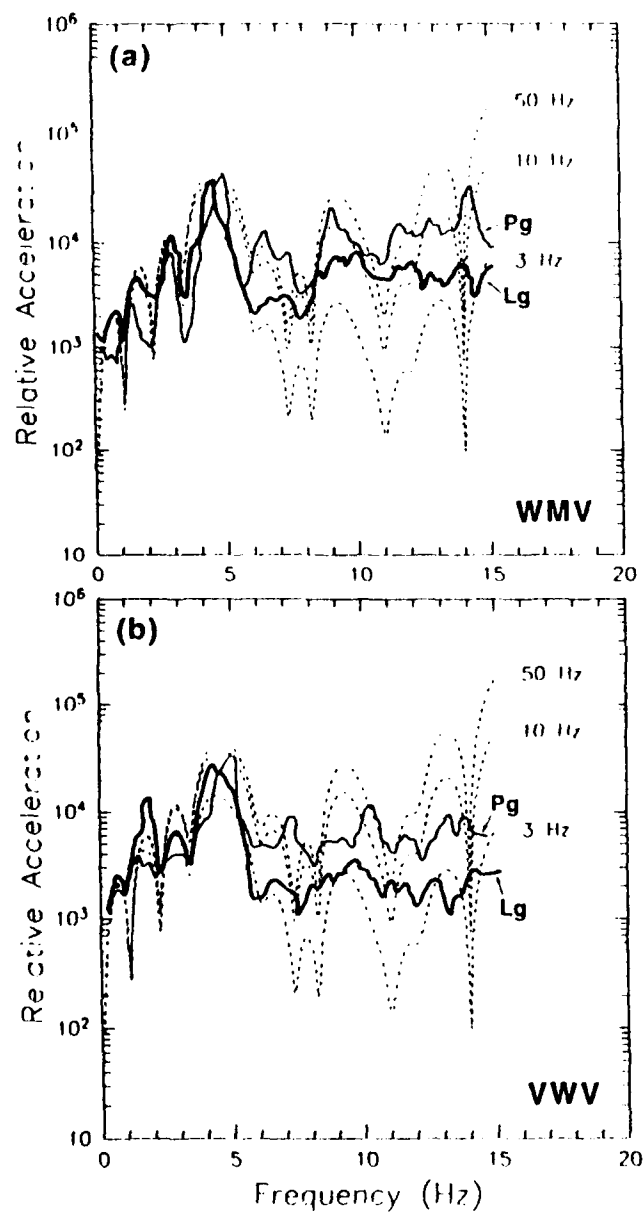


Fig. 8. Pg (thin line) and Lg (thick line) acceleration spectra for explosion 1 at stations WMV (a) and VWV (b). Dashed lines show model spectra for three different source corner frequencies. The observed spectra have been shifted vertically for comparison.

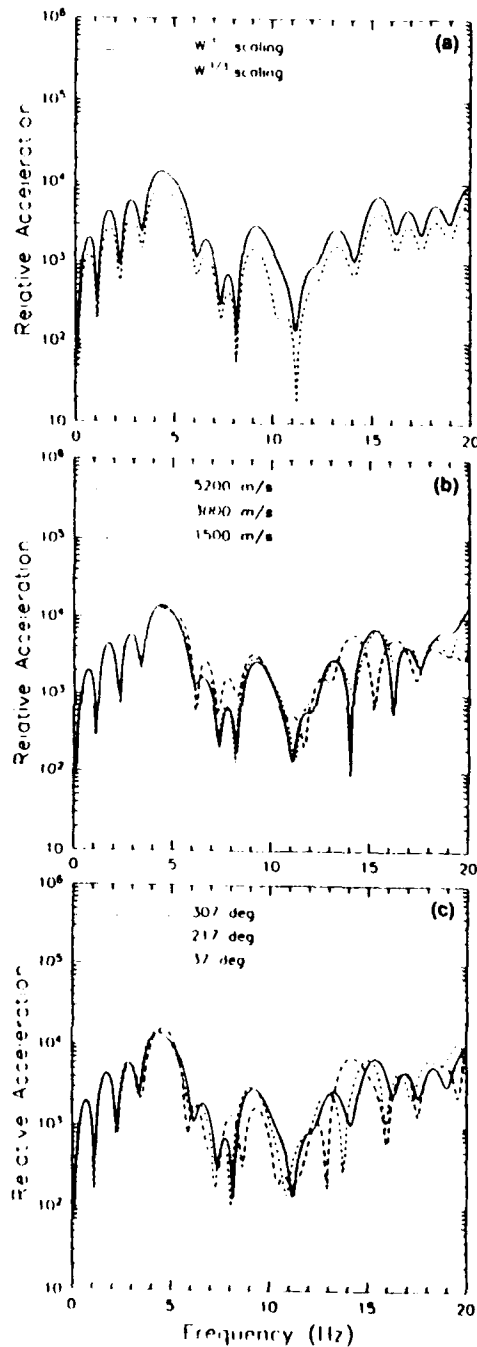


Fig. 9. Model acceleration spectra for Explosion 1 assuming: (a) amplitude scaling proportional to the charge weight (solid line) and cube root of charge weight (dashed line); (b) 3 different values of phase velocity (azimuth 307 deg); (c) 3 different values of station azimuth (phase velocity 3000 m/sec).

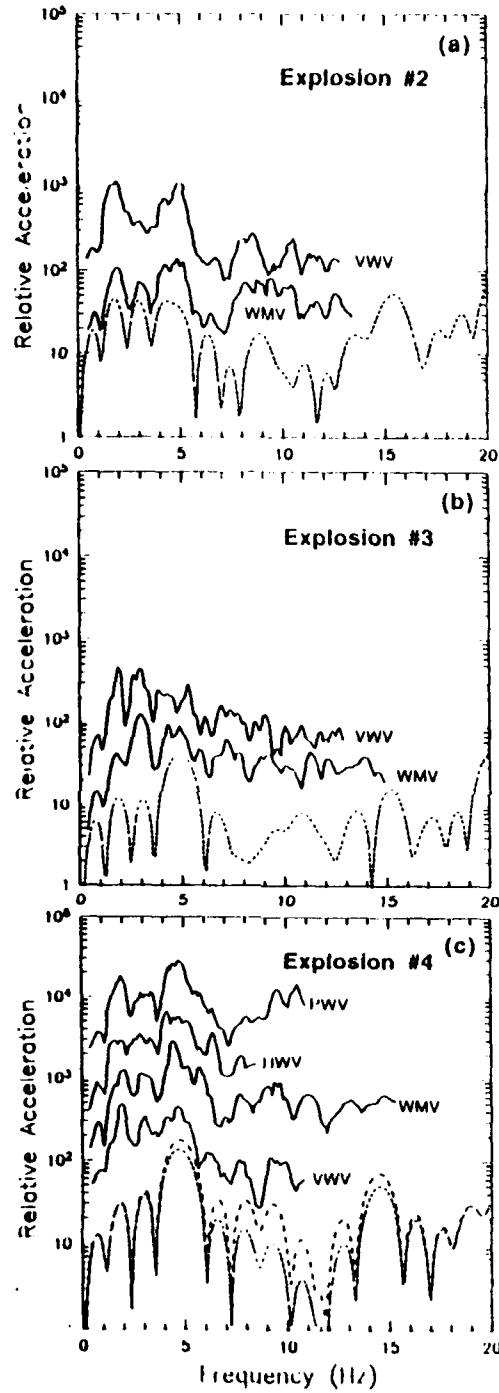


Fig. 10. Vertical component Lg acceleration spectra for Explosions 2, 3 and 4 are shown by solid lines in (a), (b) and (c), respectively. Short dashed lines show the model spectra, assuming that explosions were decked. The long dashed line in (c) shows the model spectrum for an undecked explosion. Amplitudes have been scaled for separation.



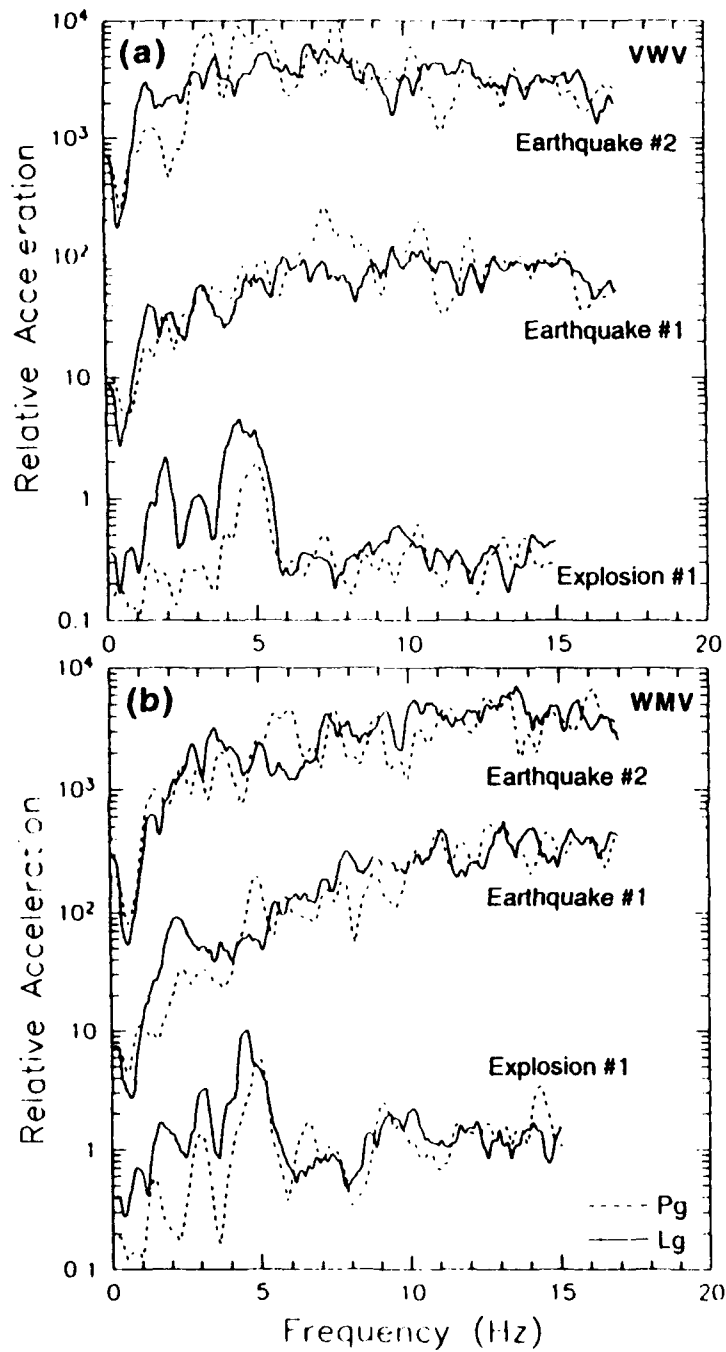


Fig. 11. (a) Vertical component Lg acceleration spectra at VWV for Earthquake 2 (Aug. 17, 1990); Earthquake 1, (Nov. 27, 1987); and Explosion 1. Solid lines show Lg spectra (20 sec windows); Dashed lines show Pg spectra (6 sec windows). (b) same as in (a) for station VWV.

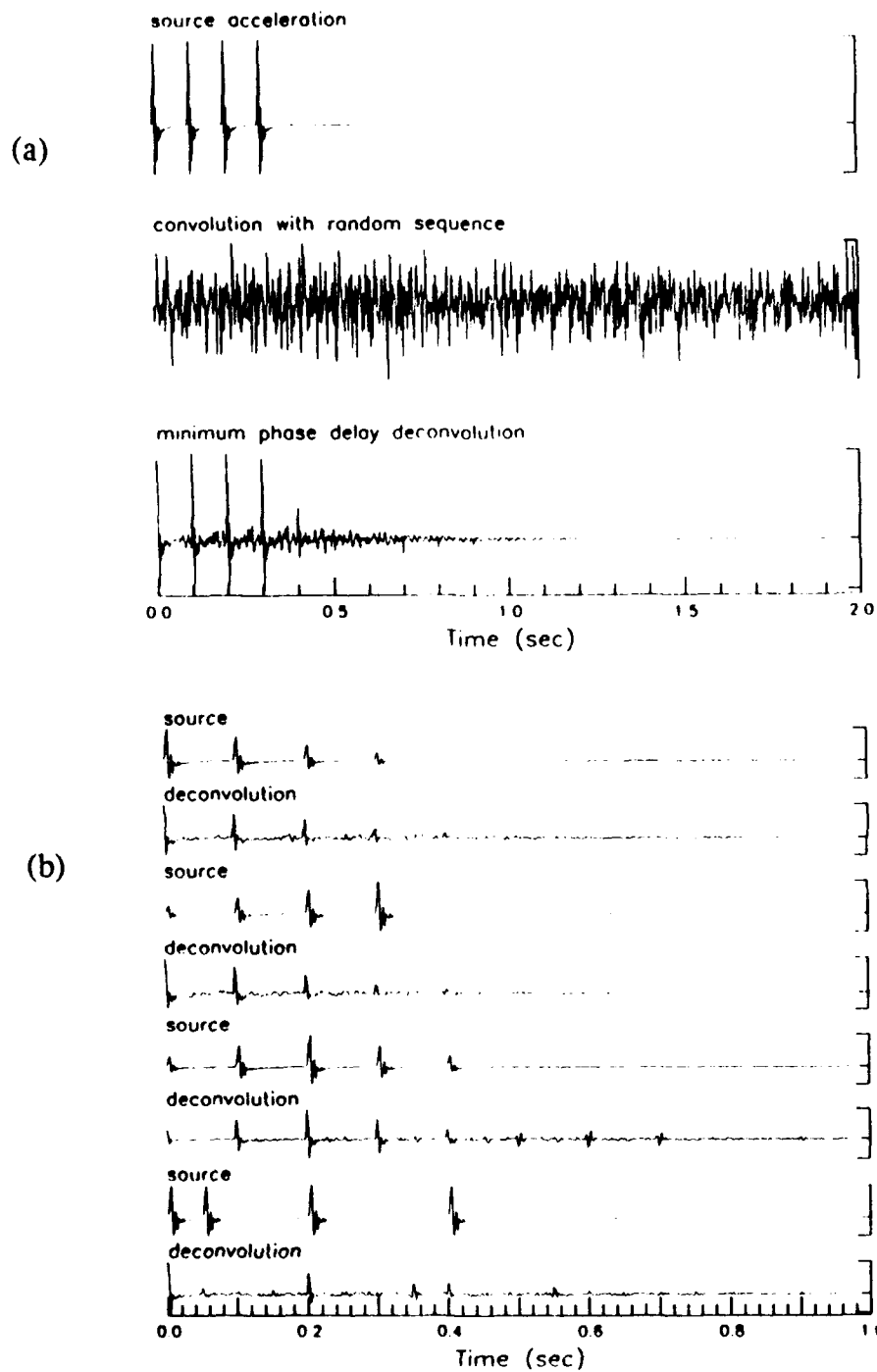


Fig. 12. (a) Example deconvolution: (top) Synthetic source time series. (middle) Simulated seismic trace obtained by convolution with a random sequence. (bottom) Result of minimum phase deconvolution. (b) Four examples of minimum phase deconvolutions, with different source time series.

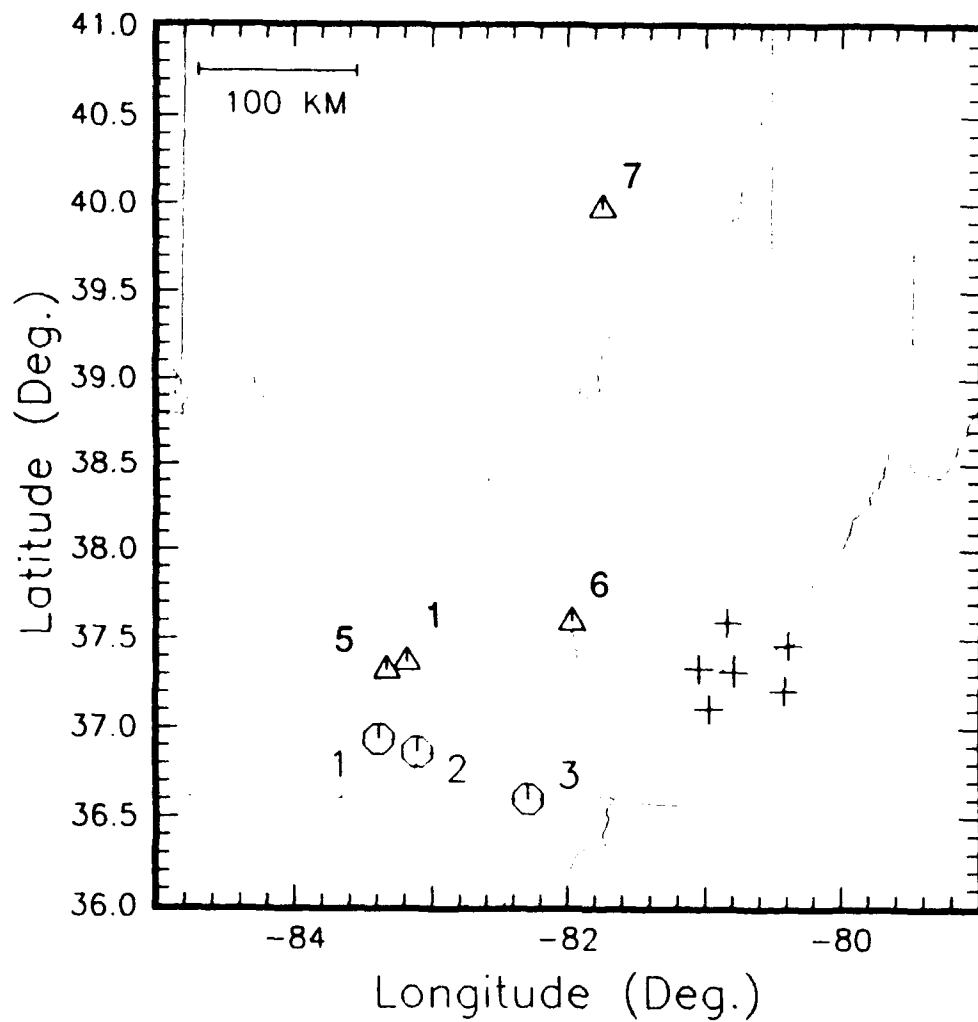


Fig. 13. Map showing locations of explosions (triangles) and earthquakes (circles) used in the deconvolution analysis. Note: Explosion 1 and Earthquakes 1 and 2 are also shown in Figure 3.

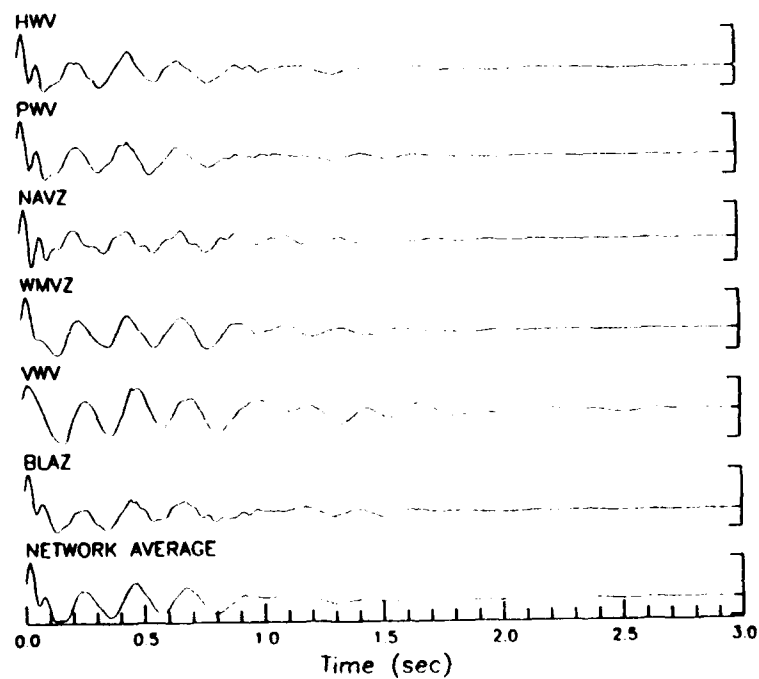
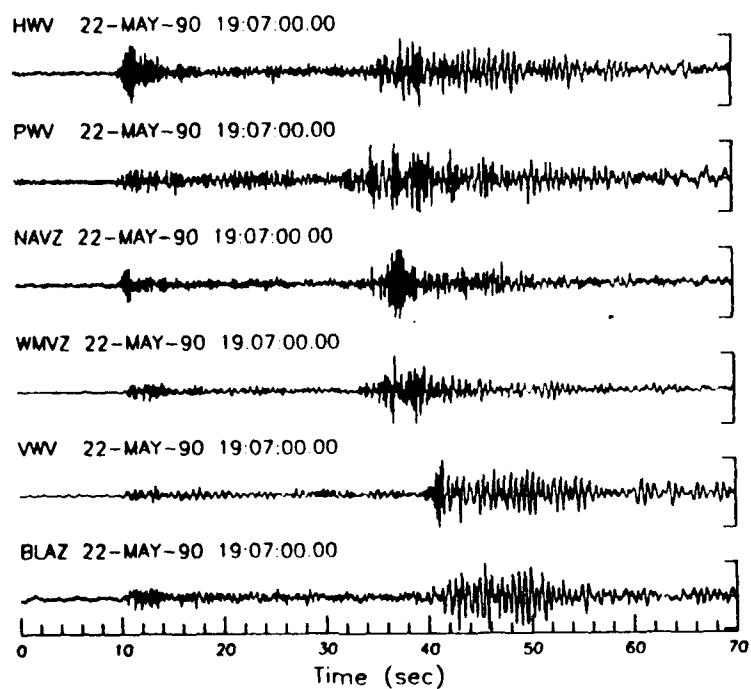


Fig. 14. Time series and minimum phase deconvolutions for Explosion 1.

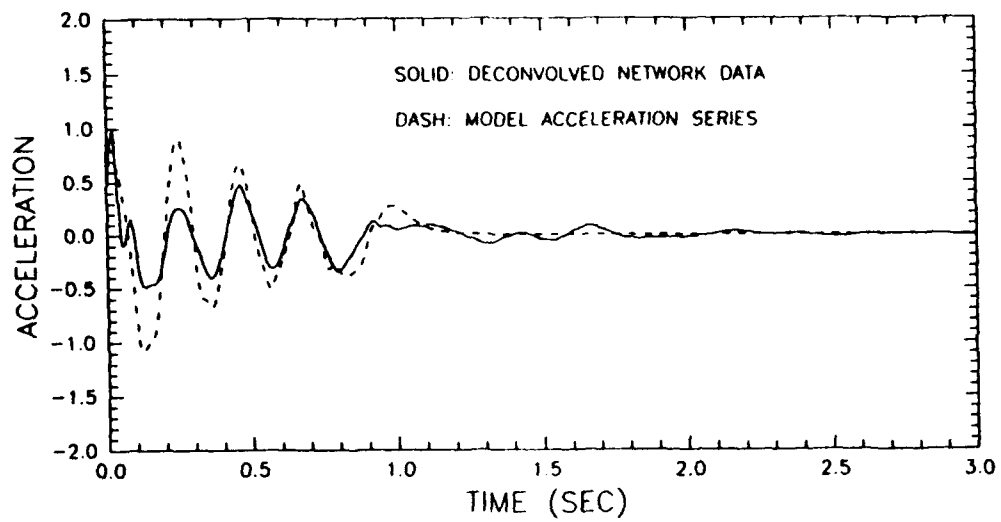


Fig. 15. Comparison of network average deconvolution with the model source acceleration time series for Explosion 1.

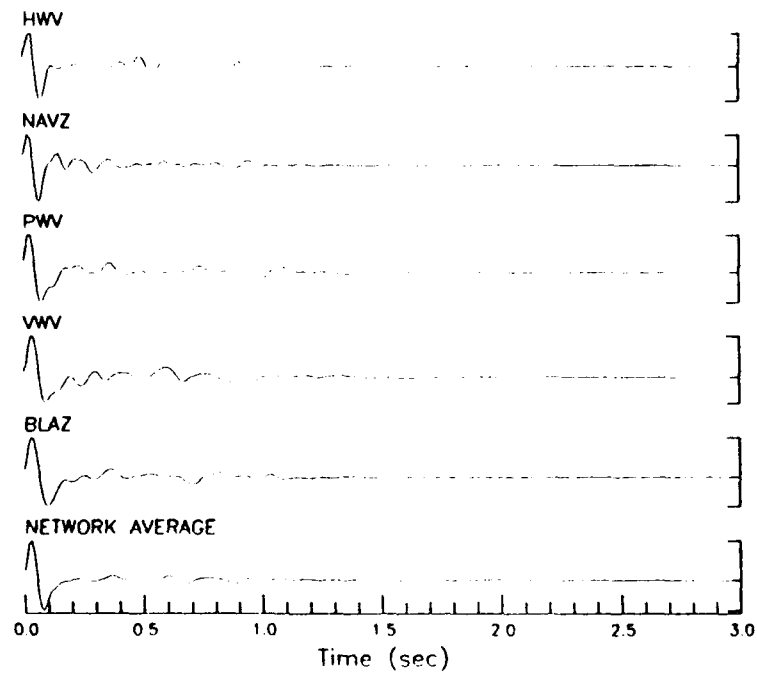
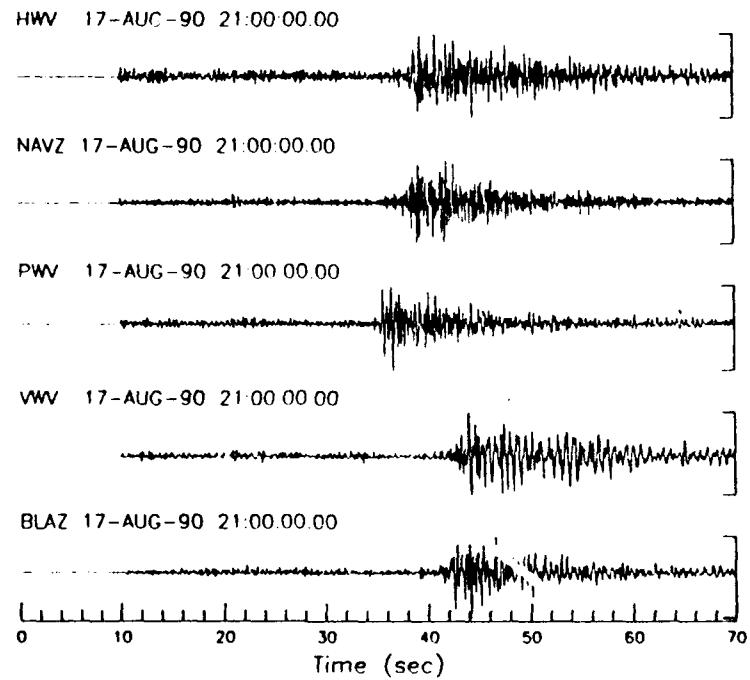


Fig. 16. Time series and deconvolution results for Earthquake 1.

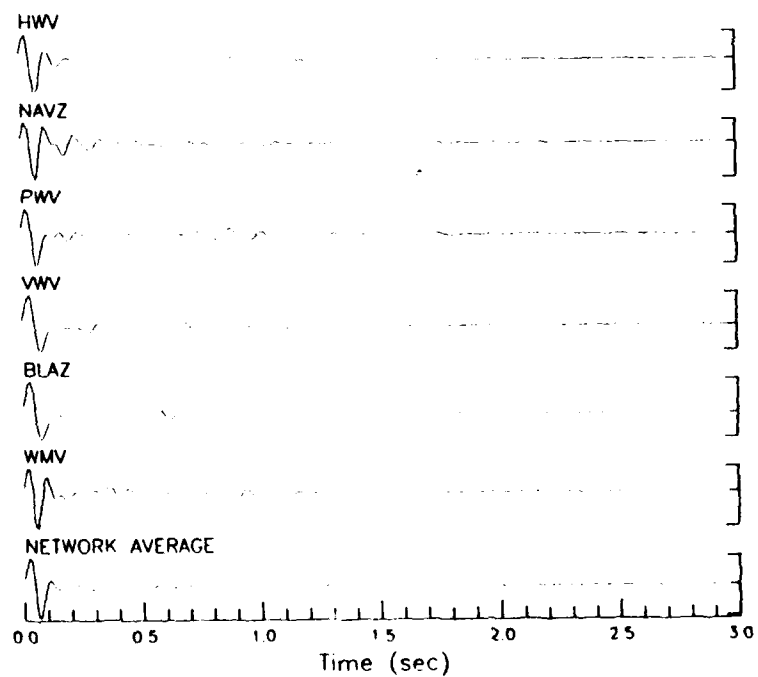
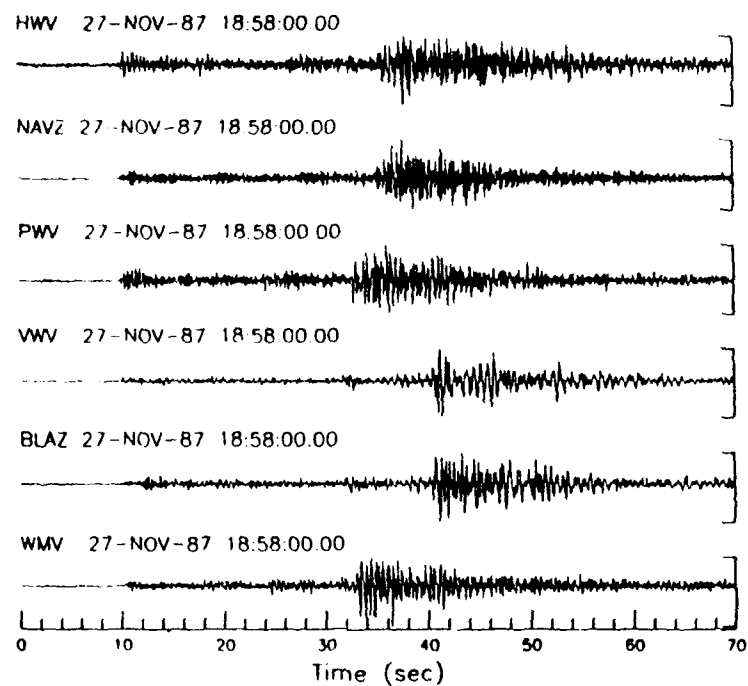


Fig. 17. Time series and deconvolution results for Earthquake 2.

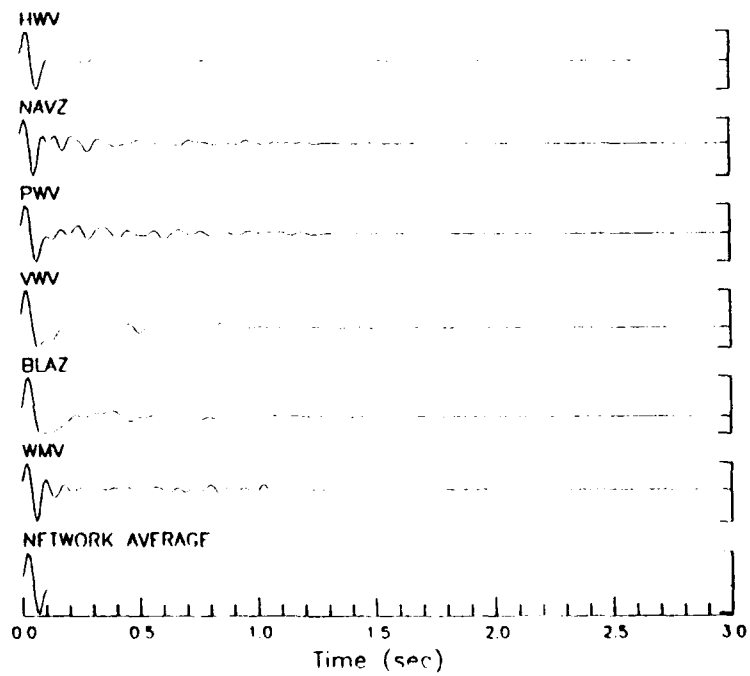
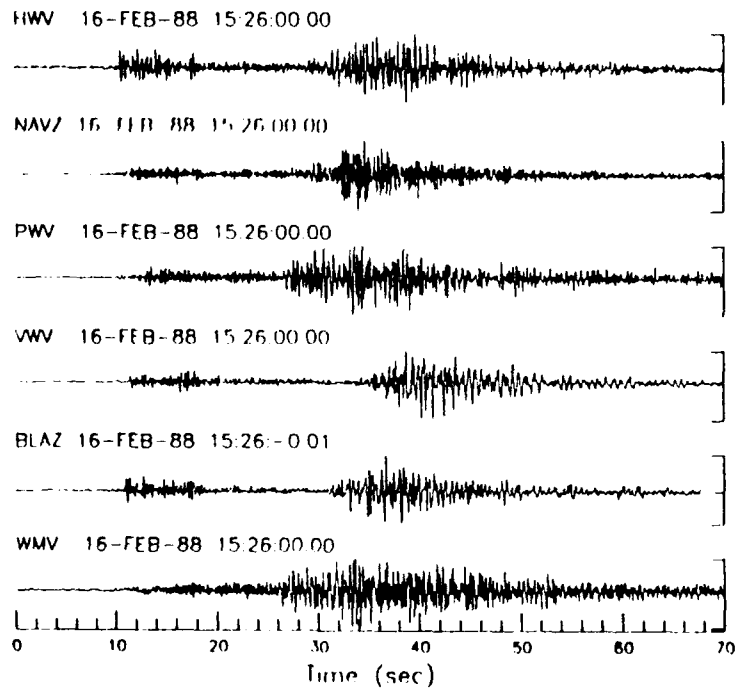


Fig. 18. Time series and deconvolution results for Earthquake 3.



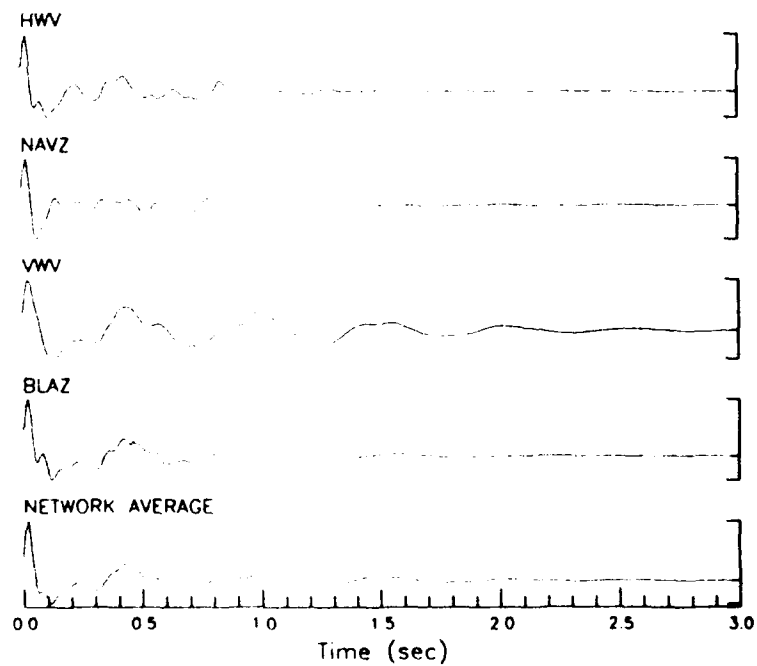
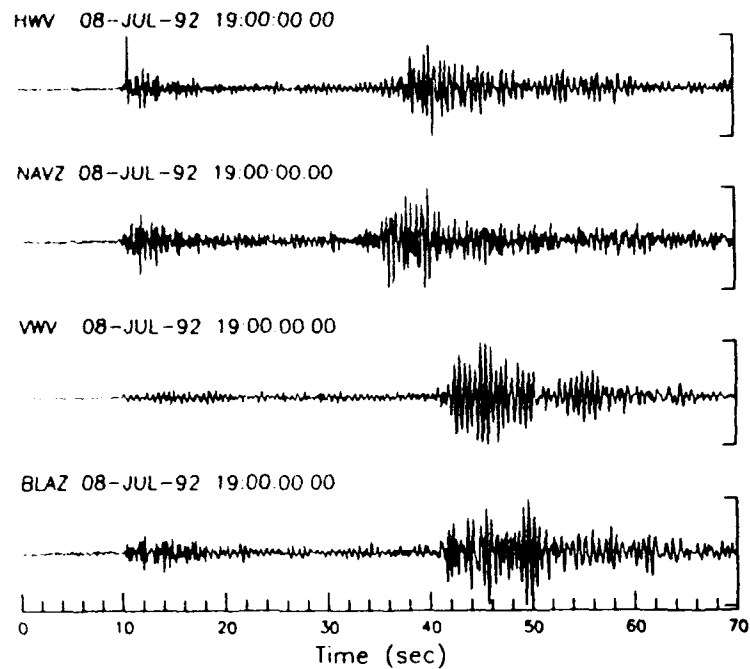


Fig. 19. Time series and deconvolution results for Explosion 5.

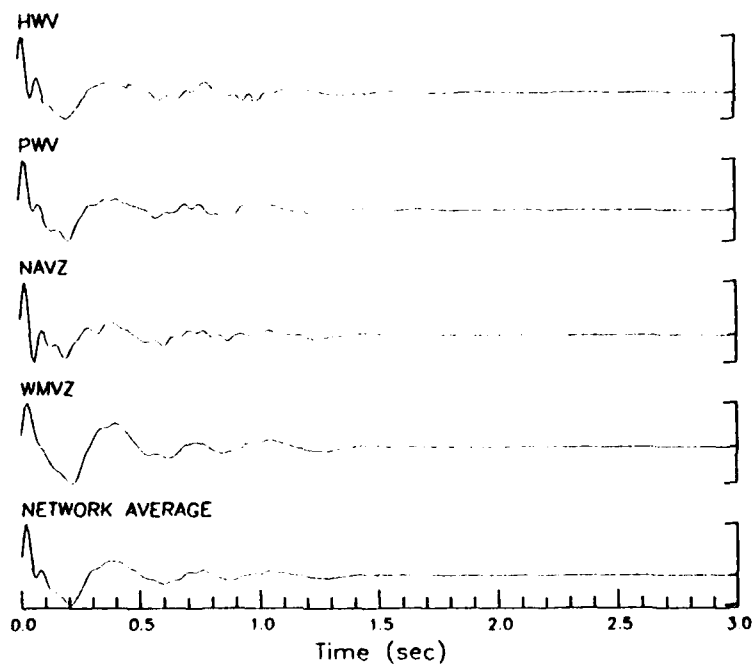
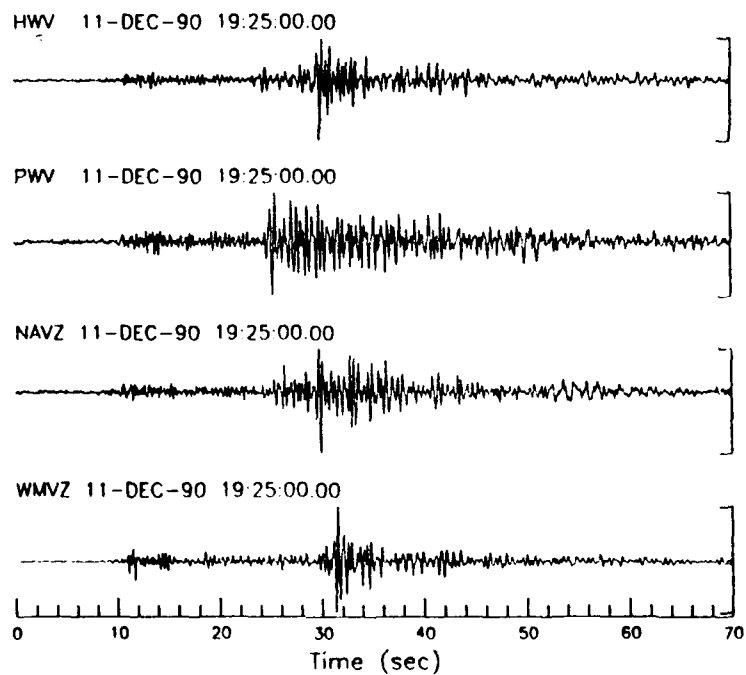


Fig. 20. Time series and deconvolution results for Explosion 6.

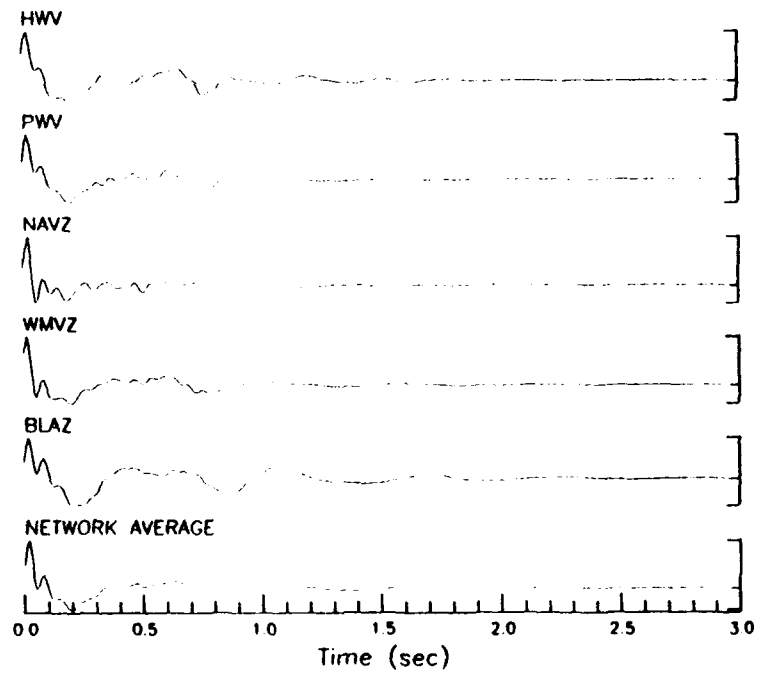
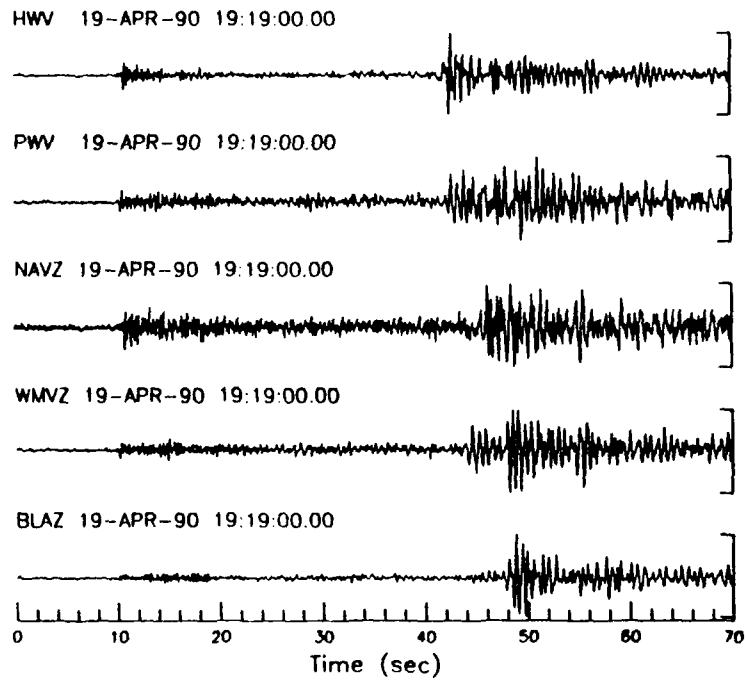


Fig. 21. Time series and deconvolution results for Explosion 7.

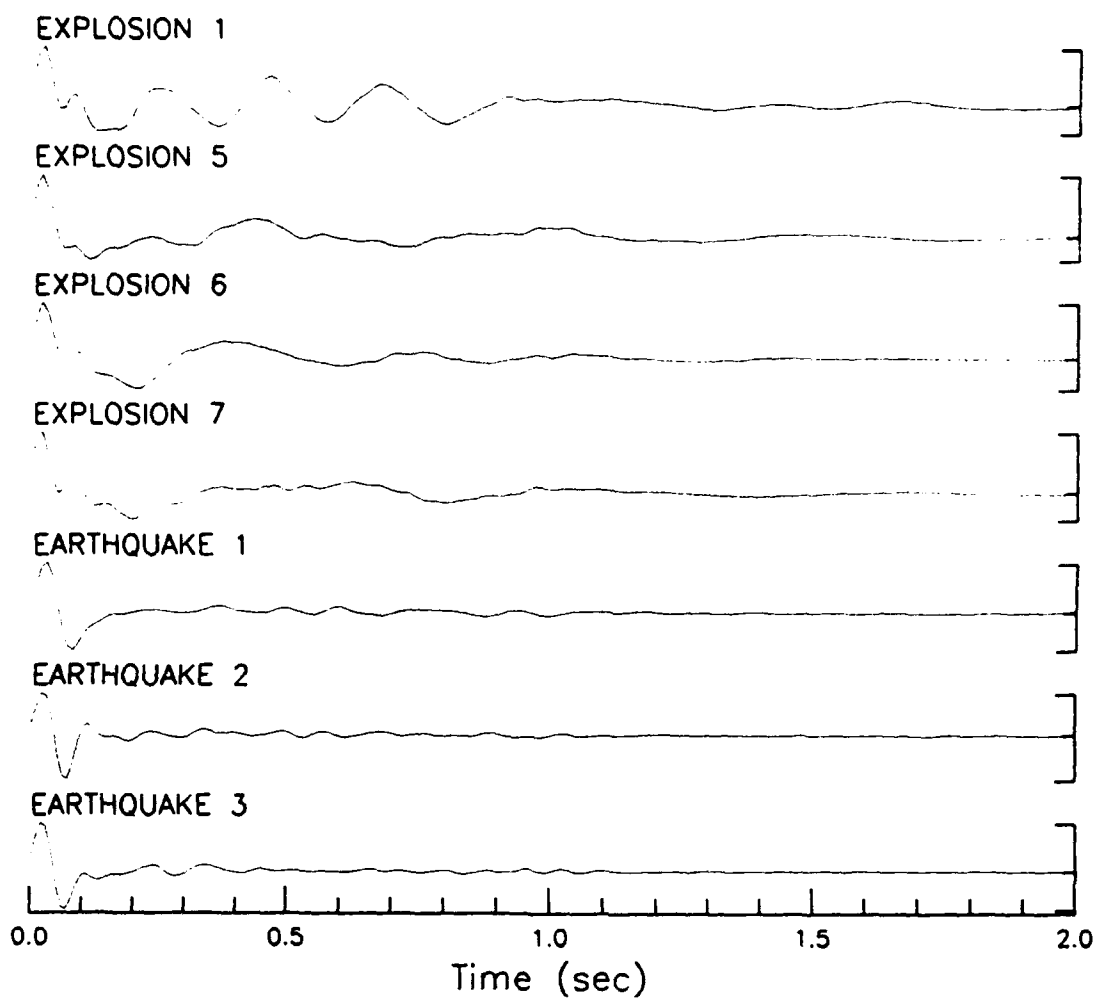


Fig. 22. Network average deconvolved acceleration series for all events in Figure 13.

Prof. Thomas Ahrens  
Seismological Lab, 252-21  
Division of Geological & Planetary Sciences  
California Institute of Technology  
Pasadena, CA 91125

- Prof. Keiiti Aki  
Center for Earth Sciences  
University of Southern California
- University Park  
Los Angeles, CA 90089-0741

Prof. Shelton Alexander  
Geosciences Department  
403 Deike Building  
The Pennsylvania State University  
University Park, PA 16802

Dr. Ralph Alewine, III  
DARPA/NMRO  
3701 North Fairfax Drive  
Arlington, VA 22203-1714

Prof. Charles B. Archambeau  
CIRES  
University of Colorado  
Boulder, CO 80309

Dr. Thomas C. Bache, Jr.  
Science Applications Int'l Corp.  
10260 Campus Point Drive  
San Diego, CA 92121 (2 copies)

Prof. Muawia Barazangi  
Institute for the Study of the Continent  
Cornell University  
Ithaca, NY 14853

Dr. Jeff Barker  
Department of Geological Sciences  
State University of New York  
at Binghamton  
• Vestal, NY 13901

Dr. Douglas R. Baumgardt  
• ENSCO, Inc  
5400 Port Royal Road  
Springfield, VA 22151-2388

Dr. Susan Beck  
Department of Geosciences  
Building #77  
University of Arizona  
Tucson, AZ 85721

Dr. T.J. Bennett  
S-CUBED  
A Division of Maxwell Laboratories  
11800 Sunrise Valley Drive, Suite 1212  
Reston, VA 22091

Dr. Robert Blandford  
AFTAC/TT, Center for Seismic Studies  
1300 North 17th Street  
Suite 1450  
Arlington, VA 22209-2308

Dr. Stephen Bratt  
Center for Seismic Studies  
1300 North 17th Street  
Suite 1450  
Arlington, VA 22209-2308

Dr. Lawrence Burdick  
Woodward-Clyde Consultants  
566 El Dorado Street  
Pasadena, CA 91109-3245

Dr. Robert Burrige  
Schlumberger-Doll Research Center  
Old Quarry Road  
Ridgefield, CT 06877

Dr. Jerry Carter  
Center for Seismic Studies  
1300 North 17th Street  
Suite 1450  
Arlington, VA 22209-2308

Dr. Eric Chael  
Division 9241  
Sandia Laboratory  
Albuquerque, NM 87185

Dr. Martin Chapman  
Department of Geological Sciences  
Virginia Polytechnical Institute  
21044 Derring Hall  
Blacksburg, VA 24061

Prof. Vernon F. Cormier  
Department of Geology & Geophysics  
U-45, Room 207  
University of Connecticut  
Storrs, CT 06268

Prof. Steven Day  
Department of Geological Sciences  
San Diego State University  
San Diego, CA 92182

Marvin Denny  
U.S. Department of Energy  
Office of Arms Control  
Washington, DC 20585

Dr. Cliff Frolich  
Institute of Geophysics  
8701 North Mopac  
Austin, TX 78759

Dr. Zoltan Der  
ENSCO, Inc.  
5400 Port Royal Road  
Springfield, VA 22151-2388

Dr. Holly Given  
IGPP, A-025  
Scripps Institute of Oceanography  
University of California, San Diego  
La Jolla, CA 92093

Prof. Adam Dziewonski  
Hoffman Laboratory, Harvard University  
Dept. of Earth Atmos. & Planetary Sciences  
20 Oxford Street  
Cambridge, MA 02138

Dr. Jeffrey W. Given  
SAIC  
10260 Campus Point Drive  
San Diego, CA 92121

Prof. John Ebel  
Department of Geology & Geophysics  
Boston College  
Chestnut Hill, MA 02167

Dr. Dale Glover  
Defense Intelligence Agency  
ATTN: ODT-1B  
Washington, DC 20301

Eric Fielding  
SNEE Hall  
INSTOC  
Cornell University  
Ithaca, NY 14853

Dr. Indra Gupta  
Teledyne Geotech  
314 Montgomery Street  
Alexandria, VA 22314

Dr. Mark D. Fisk  
Mission Research Corporation  
735 State Street  
P.O. Drawer 719  
Santa Barbara, CA 93102

Dan N. Hagedorn  
Pacific Northwest Laboratories  
Battelle Boulevard  
Richland, WA 99352

Prof Stanley Flatte  
Applied Sciences Building  
University of California, Santa Cruz  
Santa Cruz, CA 95064

Dr. James Hannon  
Lawrence Livermore National Laboratory  
P.O. Box 808  
L-205  
Livermore, CA 94550

Dr. John Foley  
NER-Geo Sciences  
1100 Crown Colony Drive  
Quincy, MA 02169

Dr. Roger Hansen  
HQ AFTAC/TTR  
Patrick AFB, FL 32925-6001

Prof. Donald Forsyth  
Department of Geological Sciences  
Brown University  
Providence, RI 02912

Prof. David G. Harkrider  
Seismological Laboratory  
Division of Geological & Planetary Sciences  
California Institute of Technology  
Pasadena, CA 91125

Dr. Art Frankel  
U.S. Geological Survey  
922 National Center  
Reston, VA 22092

Prof. Danny Harvey  
CIRES  
University of Colorado  
Boulder, CO 80309

Prof. Donald V. Helmberger  
Seismological Laboratory  
Division of Geological & Planetary Sciences  
California Institute of Technology  
Pasadena, CA 91125

• Prof. Eugene Herrin  
Institute for the Study of Earth and Man  
Geophysical Laboratory  
Southern Methodist University  
• Dallas, TX 75275

Prof. Robert B. Herrmann  
Department of Earth & Atmospheric Sciences  
St. Louis University  
St. Louis, MO 63156

Prof. Lane R. Johnson  
Seismographic Station  
University of California  
Berkeley, CA 94720

Prof. Thomas H. Jordan  
Department of Earth, Atmospheric &  
Planetary Sciences  
Massachusetts Institute of Technology  
Cambridge, MA 02139

Prof. Alan Kafka  
Department of Geology & Geophysics  
Boston College  
Chestnut Hill, MA 02167

Robert C. Kemerait  
ENSCO, Inc.  
445 Pineda Court  
Melbourne, FL 32940

Dr. Karl Koch  
Institute for the Study of Earth and Man  
Geophysical Laboratory  
Southern Methodist University  
Dallas, Tx 75275

• Dr. Max Koontz  
U.S. Dept. of Energy/DP 5  
• Forrestal Building  
1000 Independence Avenue  
Washington, DC 20585

Dr. Richard LaCoss  
MIT Lincoln Laboratory, M-200B  
P.O. Box 73  
Lexington, MA 02173-0073

Dr. Fred K. Lamb  
University of Illinois at Urbana-Champaign  
Department of Physics  
1110 West Green Street  
Urbana, IL 61801

Prof. Charles A. Langston  
Geosciences Department  
403 Deike Building  
The Pennsylvania State University  
University Park, PA 16802

Jim Lawson, Chief Geophysicist  
Oklahoma Geological Survey  
Oklahoma Geophysical Observatory  
P.O. Box 8  
Leonard, OK 74043-0008

Prof. Thorne Lay  
Institute of Tectonics  
Earth Science Board  
University of California, Santa Cruz  
Santa Cruz, CA 95064

Dr. William Leith  
U.S. Geological Survey  
Mail Stop 928  
Reston, VA 22092

Mr. James F. Lewkowicz  
Phillips Laboratory/GPEH  
Hanscom AFB, MA 01731-5000( 2 copies)

Mr. Alfred Lieberman  
ACDA/VI-OA State Department Building  
Room 5726  
320-21st Street, NW  
Washington, DC 20451

Prof. L. Timothy Long  
School of Geophysical Sciences  
Georgia Institute of Technology  
Atlanta, GA 30332

Dr. Randolph Martin, III  
New England Research, Inc.  
76 Olcott Drive  
White River Junction, VT 05001

Dr. Robert Masse  
Denver Federal Building  
Box 25046, Mail Stop 967  
Denver, CO 80225

Dr. Gary McCartor  
Department of Physics  
Southern Methodist University  
Dallas, TX 75275

Prof. Thomas V. McEvilly  
Seismographic Station  
University of California  
Berkeley, CA 94720

Dr. Art McGarr  
U.S. Geological Survey  
Mail Stop 977  
U.S. Geological Survey  
Menlo Park, CA 94025

Dr. Keith L. McLaughlin  
S-CUBED  
A Division of Maxwell Laboratory  
P.O. Box 1620  
La Jolla, CA 92038-1620

Stephen Miller & Dr. Alexander Florence  
SRI International  
333 Ravenswood Avenue  
Box AF 116  
Menlo Park, CA 94025-3493

Prof. Bernard Minster  
IGPP, A-025  
Scripps Institute of Oceanography  
University of California, San Diego  
La Jolla, CA 92093

Prof. Brian J. Mitchell  
Department of Earth & Atmospheric Sciences  
St. Louis University  
St. Louis, MO 63156

Mr. Jack Murphy  
S-CUBED  
A Division of Maxwell Laboratory  
11800 Sunrise Valley Drive, Suite 1212  
Reston, VA 22091 (2 Copies)

Dr. Keith K. Nakanishi  
Lawrence Livermore National Laboratory  
L-025  
P.O. Box 808  
Livermore, CA 94550

Dr. Carl Newton  
Los Alamos National Laboratory  
P.O. Box 1663  
Mail Stop C335, Group ESS-3  
Los Alamos, NM 87545

Dr. Bao Nguyen  
HQ AFTAC/TTR  
Patrick AFB, FL 32925-6001

Prof. John A. Orcutt  
IGPP, A-025  
Scripps Institute of Oceanography  
University of California, San Diego  
La Jolla, CA 92093

Prof. Jeffrey Park  
Kline Geology Laboratory  
P.O. Box 6666  
New Haven, CT 06511-8130

Dr. Howard Patton  
Lawrence Livermore National Laboratory  
L-025  
P.O. Box 808  
Livermore, CA 94550

Dr. Frank Pilotte  
HQ AFTAC/TT  
Patrick AFB, FL 32925-6001

Dr. Jay J. Pulli  
Kadix Systems, Inc.  
2 Taft Court, Suite 203  
Rockville, MD 20850

Dr. Robert Reinke  
ATTN: FCTVTD  
Field Command  
Defense Nuclear Agency  
Kirtland AFB, NM 87115

Prof. Paul G. Richards  
Lamont-Doherty Geological Observatory  
of Columbia University  
Palisades, NY 10964

Mr. Wilmer Rivers  
Teledyne Geotech  
314 Montgomery Street  
Alexandria, VA 22314

Dr. George Rothe  
HQ AFTAC/TTR  
Patrick AFB, FL 32925-6001



Dr. Alan S. Ryall, Jr.  
DARPA/NMRO  
3701 North Fairfax Drive  
Arlington, VA 22209-1714

• Dr. Richard Sailor  
TASC, Inc.  
55 Walkers Brook Drive  
• Reading, MA 01867

Prof. Charles G. Sammis  
Center for Earth Sciences  
University of Southern California  
University Park  
Los Angeles, CA 90089-0741

Prof. Christopher H. Scholz  
Lamont-Doherty Geological Observatory  
of Columbia University  
Palisades, NY 10964

Dr. Susan Schwartz  
Institute of Tectonics  
1156 High Street  
Santa Cruz, CA 95064

Secretary of the Air Force  
(SAFRD)  
Washington, DC 20330

Office of the Secretary of Defense  
DDR&E  
Washington, DC 20330

Thomas J. Sereno, Jr.  
Science Application Int'l Corp.  
10260 Campus Point Drive  
San Diego, CA 92121

• Dr. Michael Shore  
• Defense Nuclear Agency/SPSS  
6801 Telegraph Road  
Alexandria, VA 22310

Dr. Robert Shumway  
University of California Davis  
Division of Statistics  
Davis, CA 95616

Dr. Matthew Sibol  
Virginia Tech  
Seismological Observatory  
4044 Derring Hall  
Blacksburg, VA 24061-0420

Prof. David G. Simpson  
IRIS, Inc.  
1616 North Fort Myer Drive  
Suite 1440  
Arlington, VA 22209

Donald L. Springer  
Lawrence Livermore National Laboratory  
L-025  
P.O. Box 808  
Livermore, CA 94550

Dr. Jeffrey Stevens  
S-CUBED  
A Division of Maxwell Laboratory  
P.O. Box 1620  
La Jolla, CA 92038-1620

Lt. Col. Jim Stobie  
ATTN: AFOSR/NL  
Bolling AFB  
Washington, DC 20332-6448

Prof. Brian Stump  
Institute for the Study of Earth & Man  
Geophysical Laboratory  
Southern Methodist University  
Dallas, TX 75275

Prof. Jeremiah Sullivan  
University of Illinois at Urbana-Champaign  
Department of Physics  
1110 West Green Street  
Urbana, IL 61801

Prof. L. Sykes  
Lamont-Doherty Geological Observatory  
of Columbia University  
Palisades, NY 10964

Dr. David Taylor  
ENSCO, Inc.  
445 Pineda Court  
Melbourne, FL 32940

Dr. Steven R. Taylor  
Los Alamos National Laboratory  
P.O. Box 1663  
Mail Stop C335  
Los Alamos, NM 87545

Prof. Clifford Thurber  
University of Wisconsin-Madison  
Department of Geology & Geophysics  
1215 West Dayton Street  
Madison, WI 53706

Prof. M. Nafi Toksoz  
Earth Resources Lab  
Massachusetts Institute of Technology  
42 Carleton Street  
Cambridge, MA 02142

Dr. Larry Turnbull  
CIA-OSWR/NED  
Washington, DC 20505

Dr. Gregory van der Vink  
IRIS, Inc.  
1616 North Fort Myer Drive  
Suite 1440  
Arlington, VA 22209

Dr. Karl Veith  
EG&G  
5211 Auth Road  
Suite 240  
Suitland, MD 20746

Prof. Terry C. Wallace  
Department of Geosciences  
Building #77  
University of Arizona  
Tucson, AZ 85721

Dr. Thomas Weaver  
Los Alamos National Laboratory  
P.O. Box 1663  
Mail Stop C335  
Los Alamos, NM 87545

Dr. William Wortman  
Mission Research Corporation  
8560 Cinderbed Road  
Suite 700  
Newington, VA 22122

Prof. Francis T. Wu  
Department of Geological Sciences  
State University of New York  
at Binghamton  
Vestal, NY 13901

AFTAC/CA  
(STINFO)  
Patrick AFB, FL 32925-6001

DARPA/PM  
3701 North Fairfax Drive  
Arlington, VA 22203-1714

DARPA/RMO/RETRIEVAL  
3701 North Fairfax Drive  
Arlington, VA 22203-1714

DARPA/RMO/SECURITY OFFICE  
3701 North Fairfax Drive  
Arlington, VA 22203-1714

HQ DNA  
ATTN: Technical Library  
Washington, DC 20305

Defense Intelligence Agency  
Directorate for Scientific & Technical Intelligence  
ATTN: DTIB  
Washington, DC 20340-6158

Defense Technical Information Center  
Cameron Station  
Alexandria, VA 22314 (2 Copies)

TACTEC  
Battelle Memorial Institute  
505 King Avenue  
Columbus, OH 43201 (Final Report)

Phillips Laboratory  
ATTN: XPG  
Hanscom AFB, MA 01731-5000

Phillips Laboratory  
ATTN: GPE  
Hanscom AFB, MA 01731-5000

Phillips Laboratory  
ATTN: TSML  
Hanscom AFB, MA 01731-5000

Phillips Laboratory  
ATTN: SUL  
Kirtland, NM 87117 (2 copies)

Dr. Svein Mykkeltveit  
NTNT/NORSAR  
P.O. Box 51  
N-2007 Kjeller, NORWAY (3 Copies)

- Dr. Michel Bouchon  
I.R.I.G.M.-B.P. 68  
38402 St. Martin D'Heres  
• Cedex, FRANCE

Prof. Keith Priestley  
University of Cambridge  
Bullard Labs, Dept. of Earth Sciences  
Madingley Rise, Madingley Road  
Cambridge CB3 0EZ, ENGLAND

Dr. Michel Campillo  
Observatoire de Grenoble  
I.R.I.G.M.-B.P. 53  
38041 Grenoble, FRANCE

Dr. Jorg Schlittenhardt  
Federal Institute for Geosciences & Nat'l Res.  
Postfach 510153  
D-3000 Hannover 51, GERMANY

Dr. Kin Yip Chun  
Geophysics Division  
Physics Department  
University of Toronto  
Ontario, CANADA

Dr. Johannes Schweitzer  
Institute of Geophysics  
Ruhr University/Bochum  
P.O. Box 1102148  
4360 Bochum 1, GERMANY

Prof. Hans-Peter Harjes  
Institute for Geophysics  
Ruhr University/Bochum  
P.O. Box 102148  
4630 Bochum 1, GERMANY

Prof. Eystein Husebye  
NTNF/NORSAR  
P.O. Box 51  
N-2007 Kjeller, NORWAY

David Jepsen  
Acting Head, Nuclear Monitoring Section  
Bureau of Mineral Resources  
Geology and Geophysics  
G.P.O. Box 378, Canberra, AUSTRALIA

Ms. Eva Johannisson  
Senior Research Officer  
FOA  
S-172 90 Sundbyberg, SWEDEN

- Dr. Peter Marshall  
Procurement Executive  
• Ministry of Defense  
Blacknest, Brimpton  
Reading FG7-FRS, UNITED KINGDOM

Dr. Bernard Massinon, Dr. Pierre Mechler  
Societe Radiomana  
27 rue Claude Bernard  
75005 Paris, FRANCE (2 Copies)